by frequent (first 5-min and then 10-min intervals) measurements (32 pulses in an acquisition time of 66 s). From integrated intensities of the C_5H_5 resonances (see Figure 3), the concentrations of each species at any time were obtained. This data was used to prepare ln [A] veresus time plots. The least-squares best line was calculated for the data, and the plots were examined by using the χ^2 test. Approximate values of k_2 were obtained by examining the best fit of calculated k_1 and varied k_2 values with respect to experimental-data-derived reaction profiles. The following experiments were conducted:

1. $[\mathbf{1}]_0 = 0.0043$ M, $[t\text{-BuNC}]_0 = 0.0172$ M; $k_1 = 0.000\,56$ s^{-1} ($\chi^2 = 1.024$).

2. $[\mathbf{1}]_0 = 0.0043$ M, $[t\text{-BuNC}]_0 = 0.0258$ M; $k_1 = 0.000\,41$ s^{-1} ($\chi^2 = 1.764$).

3. $[\mathbf{1}]_0 = 0.0054$ M, $[t\text{-BuNC}]_0 = 0.0645$ M; $k_1 = 0.000\,72$ s^{-1} ($\chi^2 = 2.161$). Experiment 3 was repeated by using an internal standard of hexamethylbenzene to confirm that mass balance was preserved throughout the reaction.

X-ray Crystallography. Single crystals of $Cp_2Ru_2(MeNC)_2WS_4 \cdot CH_2Cl_2$ were obtained by layering a CH_2Cl_2 solution of the complex with pentane. The dark red, columnar crystal used for data collection was cut from a longer crystal and was observed to extinguish plane-polarized light. The crystal was mounted in a 0.3-mm thin-walled glass capillary. The crystal decomposed rapidly in the X-ray beam, but the decay was apparently an isotropic, linear function of exposure time and a correction was applied on the basis of three standard reflections, which were monitored after every 100 intensities measured (total decay ca. 65%). Data were collected at 26 °C on a Syntex $P2_1$ automated four-circle diffractometer using graphite-monochromated molybdenum radiation. Data collection parameters are presented in Table III. The data were corrected for Lorentz and polarization effects, anomalous dispersion effects, and absorption. The alternate space group setting $I2/a$ was chosen to avoid the correlations between positional parameters anticipated for the conventional *C*-centered setting where $\beta = 126.23°$.

Structure Solution and Refinement. The structure was solved by Patterson methods; correct positions for the two unique metal atoms were deduced from a sharpened Patterson map. A weighted difference Fourier synthesis gave positions for the sulfur atoms and subsequent least-squares–difference Fourier calculations revealed positions for the remaining non-hydrogen atoms (including a methylene chloride solvate molecule disordered about the 2-fold axis). The hydrogen atoms of the trimer were fixed in "idealized" positions; the hydrogen atoms of the solvate molecule were not included in the structure factor calculations. In the final cycle of least-squares refinement, all non-hydrogen atoms of the trimer and the chlorine atoms of the disordered solvate molecule were refined with anisotropic thermal coefficients, atom C8 was refined with an isotropic thermal coefficient, and a group isotropic thermal coefficient parameter was varied for the hydrogen atoms. Refinement in the acentric space group *Ia* converged with unreasonable positions for chemically equivalent atoms in the trimer and did not improve the proposed disorder model for the solvate molecule. Successful convergence of the centric least-squares refinement was indicated by the maximum shift/error for the last cycle of 0.02. In the final difference Fourier map there was no residual electron density above the background, and the highest positive peaks were in the vicinity of the metal atoms. A final analysis of variance between observed and calculated structure factors showed no obvious systematic errors. Atomic coordinates of non-hydrogen atoms and thermal parameters are presented in Tables IV and V.

Acknowledgment. This research was funded by the National Science Foundation.

Supplementary Material Available: Tables of atomic coordinates, thermal parameters, and bond lengths and angles (3 pages); a table of final observed and calculated structure factors (3 pages). Ordering information is given on any current masthead page.

Contribution from the Department of Chemistry and Biochemistry,
University of California, Los Angeles, Los Angeles, California 90024-1569

Synthesis and Structural Characterization of Copper(I) Cupracarboranes. A Novel "Pinwheel" Cluster

Han Chyul Kang, Youngkyu Do, Carolyn B. Knobler, and M. Frederick Hawthorne*

Received December 2, 1987

Synthesis and structural characteristics of copper(I) complexes of $[nido\text{-}7,8\text{-}C_2B_9H_{10}L]^{n-}$ (**1**, L = H, $n = 2$; **2**, L = 4-$(C_5H_4N)CO_2CH_3$, $n = 1$) are reported. Reaction systems with variable **1**:CuCl:PPh_3:(PPN)Cl and **2**:CuCl:PPh_3 mole ratios have resulted in the following cupracarboranes: $[closo\text{-}3\text{-}(PPh_3)\text{-}3,1,2\text{-}CuC_2B_9H_{11}]^-$ (**3**), $[closo\text{-}exo\text{-}4,8\text{-}\{(\mu\text{-}H)_2Cu(PPh_3)\}\text{-}3\text{-}(PPh_3)\text{-}3,1,2\text{-}CuC_2B_9H_9]$ (**4**), $[closo\text{-}3\text{-}(PPh_3)\text{-}4\text{-}L\text{-}3,1,2\text{-}CuC_2B_9H_{10}]$ (**5**, L = 4-$(C_5H_4N)CO_2CH_3$), and $[Cu_3(\mu\text{-}H)_3(C_2B_9H_9L)_3]$ (**6**, L = 4-$(C_5H_4N)CO_2CH_3$). These compounds have been structurally characterized by single-crystal X-ray diffraction. Crystallographic parameters are as follows (compound: crystal system; space group; crystal parameters; *Z*; unique data ($I > 3\sigma(I)$); R, R_w). PPN[**3**]: monoclinic; $P2_1/n$; $a = 11.507$ (1) Å, $b = 14.772$ (1) Å, $c = 30.751$ (2) Å, $\beta = 90.284$ (2)°; 4; 4831; 6.4, 7.6. **4**: monoclinic; $P2_1/n$; $a = 10.005$ (2) Å, $b = 20.693$ (4) Å, $c = 18.998$ (3) Å, $\beta = 92.664$ (6)°; 4; 5071; 4.5, 6.1. **5**: monoclinic; $P2_1/c$; $a = 13.798$ (1) Å, $b = 12.072$ (1) Å, $c = 18.845$ (2) Å, $\beta = 95.111$ (3)°; 4; 2290; 7.1, 8.3. **6**·n-C_7H_{16}: rhombohedral; $R\bar{3}$; $a = 17.280$ (4) Å, $c = 28.630$ (7) Å; 6; 2309; 6.5, 10.6. The polyhedral CuC_2B_9 framework is a common structural feature displayed by all four cupracarboranes. The geometry of this cage framework varies in such a way that opening of the $(d^{10}\text{-}M)C_2B_9$ icosahedra increases in the order of **3**, **4**, **5**, and **6**, resulting in closo geometry for **3** and **4**, nido geometry for **6**, and an intermediate geometry for **5**. Two copper(I) centers in **4** are associated with one carborane cage via the open pentagonal C_2B_3 face and two B–H–Cu bridges. Both bridging BH units originate from the upper pentagonal belt of the dicarbollide moiety, resulting in an interatomic Cu(I)–Cu(I) distance of 2.576 (1) Å. In a formal sense, **4** is a zwitterion composed of an anionic **3** complexed with a $[Cu(PPh_3)]^+$ cation. The dinuclear structural integrity of **4** remains intact upon dissolution, although fluxional processes become operative, as revealed by variable-temperature multinuclei FT NMR spectroscopy. The trinuclear cupracarborane **6** contains three $[CuC_2B_9H_{10}(4\text{-}(C_5H_4N)CO_2CH_3)]$ units, which are linked by both Cu–H–B and Cu–Cu (2.519 (2) Å) interactions about a crystallographic 3-fold axis such that a "pinwheel" ligand array around an equilateral Cu_3 core results. Compound **6** represents an example of a "clustered cluster". The extent of metal–metal interactions in **4** and **6**, as implied by their relatively short copper–copper distances, is discussed. Structural comparison of these copper(I) complexes suggests that the substituent at boron is not electronically "innocent" with respect to molecular distortions.

Introduction

Recent developments of the chemistry of the dicarbollide anion $[nido\text{-}7,8\text{-}C_2B_9H_{11}]^{2-}$ (**1**),[1] a unique ligand type, have proceeded with great diversity, ranging over immunological applications,[2] cluster catalysis,[3] hypervalency in nonmetals,[4] and the synthesis of clustered clusters.[5] The foregoing variety in dicarbollide

---

[1] (a) Hawthorne, M. F.; Young, D. C.; Andrews, T. D.; Howe, D. V.: Pilling, R. L.; Pitts, A. D.; Reintjes, M.; Warren, L. F., Jr.; Wegner, P. A. *J. Am. Chem. Soc.* **1968**, *90*, 879. (b) Alder, R. G.; Hawthorne, M. F. *J. Am. Chem. Soc.* **1970**, *92*, 6174.

[2] Mizusawa, E. A.; Thompson, M. R.; Hawthorne, M. F. *Inorg. Chem.* **1985**, *24*, 1911.

[3] Hawthorne, M. F. In *Chemistry for the Future, IUPAC*; Grunewald, H., Ed.; Pergamon: New York, 1984; p 135.

[4] Schubert, D. M.; Rees, W. S., Jr.; Knobler, C. B.; Hawthorne, M. F. *Pure. Appl. Chem.* **1987**, *59*, 869.

0020-1669/88/1327-1716$01.50/0 © 1988 American Chemical Society

Scheme I

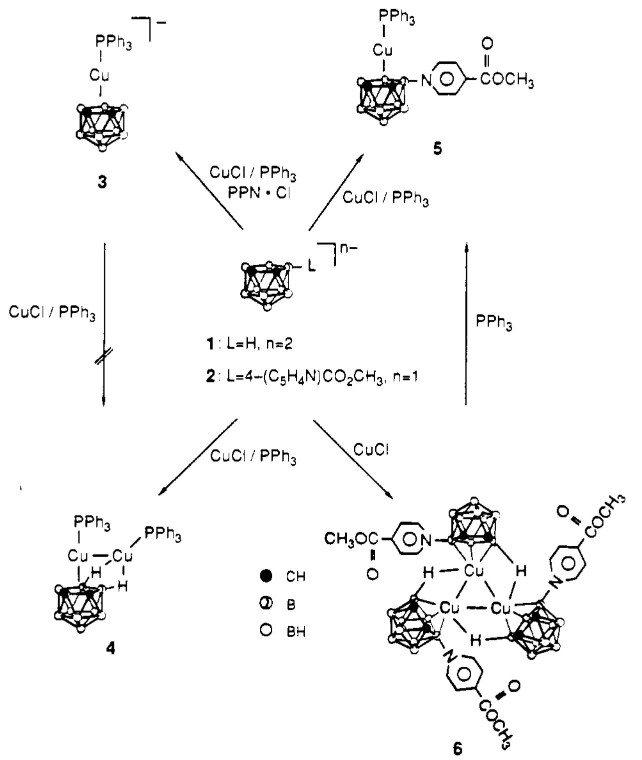

chemistry stems from the excellent electron donor ability of anion **1**. The variable ligating hapticity of the open pentagonal C_2B_3 face of **1**,[6-9] coupled with the involvement of its terminal boron-hydrogen bonds in the formation of metal-hydride-boron bridge bonds,[10] is illustrative of the structural versatility of **1** in metallacarborane chemistry.

Further modification of the chemistry of metallacarborane complexes of **1** results from the substitution of a terminal hydrogen on carbon with an alkyl or aryl group[11] or a terminal hydride on boron with a neutral Lewis base.[12] Particularly, this substitution at boron reduces the formal charge of the parent dicarbollide ion **1**, affording a monoanionic charge-compensated nido dicarbollide ion. Among the possible boron-substituted ligands, the charge-compensated dicarbollide ion [*nido*-9-(4-(C_5H_4N)CO_2CH_3)-7,8-$C_2B_9H_{10}$]$^-$ (**2**), generated by deprotonation of the oxidative-coupling product of [*nido*-7,8-$C_2B_9H_{12}$]$^-$ and methyl isonicotinate (4-(C_5H_4N)CO_2CH_3), has proven useful in the synthesis of neutral metallacarborane complexes.[13]

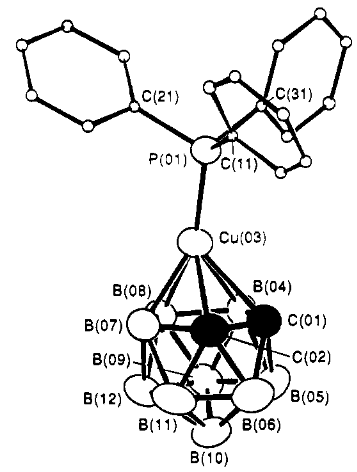

Figure 1. Molecular structure of [*closo*-3-(PPh_3)-3,1,2-$CuC_2B_9H_{11}$]$^-$ (**3**) in the PPN^+ salt showing the atom-labeling scheme. All hydrogen atoms have been omitted for clarity.

Synthesis and structural characterization of electron-rich late- and post-transition-element metallacarboranes of **1** have been of interest in order to explore the structural effect of the electron configuration of the metal in its formal oxidation state as well as the effect of the introduction of ancillary ligands onto the metal on the extent of metal-cage bonding interactions.[7,8] However, for certain elements, including formal d^{10}-Cu(I), examples of metallacarboranes are very limited or are not available. In the case of d^{10}-Cu(I), the preparation of [(PPh_3)$CuC_2B_9H_{10}$(C_5H_5N)] was reported but no X-ray structural characterization was included.[7e] Reported herein are the detailed accounts of the synthesis and structural chemistry of four new cupracarboranes containing ligands **1** and **2**, with nuclearity spanning from mononuclear to trinuclear. A portion of this work has previously been communicated.[14,15]

Results and Discussion

Synthesis. The preliminary observation that the anaerobic heterogeneous reaction system of **1**, [*nido*-7,8-$C_2B_9H_{11}$]$^{2-}$, with anhydrous copper(I) chloride was accompanied by an undesirable redox reaction[16] prompted a modification of the reaction conditions. As summarized in Scheme I, routes to novel cupracarboranes were devised by attempting to introduce factors that affect the solubilities of copper(I) reagent or reaction product(s) in solvents. With the thallium salt of **1** as a source of dicarbollide ion, mononuclear PPN[*closo*-3-(PPh_3)-3,1,2-$CuC_2B_9H_{11}$] (PPN-[**3**], PPN = bis(triphenylphosphoranylidene)ammonium) and dinuclear [*closo*-*exo*-4,8-{(μ-H)$_2$Cu(PPh_3)}-3-(PPh_3)-3,1,2-$CuC_2B_9H_9$] (**4**) can be prepared in high yield (eq 1 and 2). The

$$\mathrm{Tl}[closo\text{-}3,1,2\text{-}\mathrm{TlC_2B_9H_{11}}] + (\mathrm{PPN})\mathrm{Cl} + \mathrm{CuCl} + \mathrm{PPh_3} \xrightarrow{\mathrm{CH_3CN/CH_2Cl_2}} \underset{\mathrm{PPN}[\mathbf{3}]}{\mathrm{PPN}[closo\text{-}3\text{-}(\mathrm{PPh_3})\text{-}3,1,2\text{-}\mathrm{CuC_2B_9H_{11}}]} + 2\mathrm{TlCl} \quad (1)$$

$$\mathrm{Tl}[closo\text{-}3,1,2\text{-}\mathrm{TlC_2B_9H_{11}}] + 2\mathrm{CuCl} + 2\mathrm{PPh_3} \xrightarrow{\mathrm{CH_2Cl_2}} \underset{\mathbf{4}}{[closo\text{-}exo\text{-}4,8\text{-}\{(\mu\text{-H})_2\mathrm{Cu}(\mathrm{PPh_3})\}\text{-}3\text{-}(\mathrm{PPh_3})\text{-}3,1,2\text{-}\mathrm{CuC_2B_9H_9}]} + 2\mathrm{TlCl} \quad (2)$$

nuclearity of the product complex depends mainly on the presence

---

(5) Do, Y.; Knobler, C. B.; Hawthorne, M. F. *J. Am. Chem. Soc.* **1987**, *109*, 1853.

(6) (a) Wing, R. M. *J. Am. Chem. Soc.* **1967**, *89*, 5599. (b) Wing, R. M. *J. Am. Chem. Soc.* **1968**, *90*, 4828.

(7) (a) Colquhoun, H. M.; Greenhough, T. J.; Wallbridge, M. G. H. *J. Chem. Soc., Chem. Commun.* **1976**, 1019. (b) Colquhoun, H. M.; Greenhough, T. J.; Wallbridge, M. G. H. *J. Chem. Soc., Chem. Commun.* **1977**, 737. (c) Colquhoun, H. M.; Greenhough, T. J.; Wallbridge, M. G. H. *J. Chem. Soc., Dalton Trans.* **1978**, 303. (d) Colquhoun, H. M.; Greenhough, T. J.; Wallbridge, M. G. H. *J. Chem. Soc., Chem. Commun.* **1978**, 322. (e) Colquhoun, H. M.; Greenhough, T. J.; Wallbridge, M. G. H. *J. Chem. Soc., Dalton Trans.* **1979**, 619. (f) Colquhoun, H. M.; Greenhough, T. J.; Wallbridge, M. G. H. *J. Chem. Soc., Dalton Trans.* **1985**, 761.

(8) (a) Mingos, D. M. P.; Forsyth, M. I.; Welch, A. J. *J. Chem. Soc., Chem. Commun.* **1977**, 605. (b) Mingos, D. M. P.; Forsyth, M. I.; Welch, A. J. *J. Chem. Soc. Dalton Trans.* **1978**, 1363.

(9) Jutzi, P.; Galow, P.; Abu-Orabi, S.; Arif, A. M.; Cowley, A. H.; Norman, N. C. *Organometallics* **1987**, *6*, 1024.

(10) Grimes, R. N. In *Metal Interactions with Boron Clusters*; Grimes, R. N., Ed.; Plenum: New York, 1982; Chapter 7.

(11) (a) Paxson, T. E.; Kaloustian, M. K.; Tom, G. M.; Wiersema, R. J.; Hawthorne, M. F. *J. Am. Chem. Soc.* **1972**, *94*, 4882. (b) Callahan, K. P.; Hawthorne, M. F. *J. Am. Chem. Soc.* **1973**, *95*, 4574. (c) Knobler, C. B.; Marder, T. B.; Mizusawa, E. A.; Teller, R. G.; Long, J. A.; Behnken, P. E.; Hawthorne, M. F. *J. Am. Chem. Soc.* **1984**, *106*, 2990.

(12) (a) Young, D. C.; Howe, D. V.; Hawthorne, M. F. *J. Am. Chem. Soc.* **1969**, *91*, 859. (b) Teller, R. G.; Wilczynski, J. J.; Hawthorne, M. F. *J. Chem. Soc., Chem. Commun.* **1979**, 472.

(13) Kang, H. C.; Knobler, C. B.; Hawthorne, M. F., manuscript in preparation.

(14) Do, Y.; Kang, H. C.; Knobler, C. B.; Hawthorne, M. F. *Inorg. Chem.* **1987**, *26*, 2348.

(15) Kang, H. C.; Do, Y.; Knobler, C. B.; Hawthorne, M. F. *J. Am. Chem. Soc.* **1987**, *109*, 6530.

(16) The identification of the redox reaction product(s) was not attempted since the blue coloration, observed in the reaction system, is a typical indication of Cu(II) metallacarborane: (a) Reference 1a. (b) Warren, L. F., Jr.; Hawthorne, M. F. *J. Am. Chem. Soc.* **1968**, *90*, 4823.

Table I. Selected Interatomic Distances (Å) and Angles (deg) for PPN[*closo*-3-(PPh_3)-3,1,2-$CuC_2B_9H_{11}$] (PPN[**3**])

Distances			
Cu(03)–P(01)	2.147 (2)	Cu(03)–C(01)	2.316 (6)
Cu(03)–C(02)	2.317 (6)	Cu(03)–B(04)	2.181 (7)
Cu(03)–B(07)	2.167 (7)	Cu(03)–B(08)	2.116 (7)
P(01)–C(11)	1.827 (4)	P(01)–C(21)	1.825 (4)
P(01)–C(31)	1.820 (4)	C(01)–C(02)	1.586 (9)
C(01)–B(04)	1.668 (10)	C(01)–B(05)	1.669 (10)
C(01)–B(06)	1.717 (11)	C(02)–B(06)	1.729 (10)
C(02)–B(07)	1.664 (10)	C(02)–B(11)	1.688 (11)
B(04)–B(05)	1.781 (11)	B(04)–B(08)	1.781 (10)
B(04)–B(09)	1.770 (10)	B(05)–B(06)	1.736 (11)
B(05)–B(09)	1.756 (11)	B(05)–B(10)	1.753 (12)
B(06)–B(10)	1.728 (12)	B(06)–B(11)	1.749 (12)
B(07)–B(08)	1.754 (11)	B(07)–B(11)	1.803 (11)
B(07)–B(12)	1.768 (10)	B(08)–B(09)	1.780 (10)
B(08)–B(12)	1.777 (11)	B(09)–B(10)	1.785 (12)
B(09)–B(12)	1.774 (11)	B(10)–B(11)	1.761 (11)
B(10)–B(12)	1.762 (12)	B(11)–B(12)	1.757 (12)
P–N (PPN)	1.582 (5)	P–N (PPN)	1.569 (5)
Angles			
P(01)–Cu(03)–C(01)	125.4 (2)	P(01)–Cu(03)–C(02)	127.0 (2)
P(01)–Cu(03)–B(04)	137.8 (2)	P(01)–Cu(03)–B(07)	127.0 (2)
P(01)–Cu(03)–B(08)	155.5 (2)	C(01)–Cu(03)–C(02)	40.0 (2)
C(01)–Cu(03)–B(04)	43.4 (2)	C(01)–Cu(03)–B(07)	73.4 (2)
C(01)–Cu(03)–B(08)	76.5 (2)	C(02)–Cu(03)–B(04)	73.4 (2)
C(02)–Cu(03)–B(07)	43.4 (2)	C(02)–Cu(03)–B(08)	76.3 (3)
B(04)–Cu(03)–B(07)	80.2 (3)	B(04)–Cu(03)–B(08)	49.0 (3)
B(07)–Cu(03)–B(08)	48.3 (3)	Cu(03)–P(01)–C(11)	117.7 (2)
Cu(03)–P(01)–C(21)	111.9 (1)	Cu(03)–P(01)–C(31)	114.7 (2)
C(11)–P(01)–C(21)	103.5 (2)	C(11)–P(01)–C(31)	101.6 (2)
C(21)–P(01)–C(31)	106.1 (2)	C(02)–C(01)–B(04)	111.5 (5)
C(01)–C(02)–B(07)	111.2 (5)	C(01)–B(04)–B(08)	105.6 (5)
B(06)–B(05)–B(09)	108.8 (6)	B(05)–B(06)–B(11)	108.8 (6)
C(02)–B(07)–B(08)	106.6 (5)	B(04)–B(08)–B(07)	104.8 (5)
B(05)–B(09)–B(12)	106.6 (5)	B(06)–B(11)–B(12)	107.3 (6)
B(09)–B(12)–B(11)	108.5 (6)	P–N–P (PPN)	145.7 (3)
P(01)–Cu(03)–B(10)	162.9 (1)		

or absence of the source of countercation, since the use of mole ratios of CuCl and PPh_3 different from those shown in eq 2 also affords the complex **4** as long as (PPN)Cl is absent. On the other hand, depending on the use of triphenylphosphine, the sodium salt of the boron-substituted dicarbollide ion **2** reacts with anhydrous copper(I) chloride to form either neutral mononuclear [*closo*-3-(PPh_3)-4-(4-(C_5H_4N)CO_2CH_3)-3,1,2-$CuC_2B_9H_{10}$] (**5**) or trinuclear [$Cu_3(\mu\text{-}H)_3\{C_2B_9H_9(4\text{-}(C_5H_4N)CO_2CH_3)\}_3$] (**6**) in a yield of ca. 20% (eq 3 and 4). Structural characterization (vide infra) of all four complexes raises possibilities as to conversion of **3** and **6** to **4** and **5** in the presence of CuCl/PPh_3 and PPh_3, respectively. As observed by multinuclear FT NMR spectroscopy, the trinuclear complex **6** can only be converted to the mononuclear cupracarborane **5** at ambient temperature by the addition of triphenylphosphine to a THF solution of **6**.

$$\mathrm{Na}[\textit{nido}\text{-}9\text{-}(4\text{-}(C_5H_4N)CO_2CH_3)\text{-}7,8\text{-}C_2B_9H_{10}] + \mathrm{CuCl} + \mathrm{PPh_3} \xrightarrow{\mathrm{THF}} \underset{\mathbf{5}}{[\textit{closo}\text{-}3\text{-}(PPh_3)\text{-}4\text{-}(4\text{-}(C_5H_4N)CO_2CH_3)\text{-}3,1,2\text{-}CuC_2B_9H_{10}]} + \mathrm{NaCl} \quad (3)$$

$$3\mathrm{Na}[\textit{nido}\text{-}9\text{-}(4\text{-}(C_5H_4N)CO_2CH_3)\text{-}7,8\text{-}C_2B_9H_{10}] + 3\mathrm{CuCl} \xrightarrow{\mathrm{THF}} \underset{\mathbf{6}}{[Cu_3(\mu\text{-}H)_3\{C_2B_9H_9(4\text{-}(C_5H_4N)CO_2CH_3)\}_3]} + 3\mathrm{NaCl} \quad (4)$$

Structural Analysis. (a) Mononuclear Complexes PPN[3] and 5. The crystal structure of PPN[**3**] consists of well-separated **3** anion and PPN^+ cation. The structure of the PPN^+ cation is not unusual and will not be discussed further. The mononuclear structure of **3**, displayed in Figure 1, contains the CuC_2B_9 polyhedral framework whose atom-labeling scheme was adopted from the convention for closo geometry.

Selected interatomic distances and angles for PPN[**3**] are listed in Table I. The Cu–P distance of 2.147 (2) Å can be compared to the corresponding value of 2.135 (1) Å in the isolobal[17] analogue of **3** [(PPh_3)Cu(C_5H_5)],[18] as well as those (2.25–2.29 Å) observed in [$(PPh_3)_2CuX$] (X = BH_4,[19] B_3H_8,[20] $CF_3COCHCOCH_3$,[21] NO_3[22]) and [$\{(PPh_3)_2Cu\}_2B_{10}H_{10}$]·$CHCl_3$.[23] The copper atom lies 1.678 Å from the mean plane (±0.018 Å) of the C_2B_3 pentagonal face of the C_2B_9 cage. This distance is significantly shorter than the one found in [(PPh_3)Cu(C_5H_5)], 1.862 Å.[18] The position of phosphorus is slightly displaced toward the carbon–carbon edge of the C_2B_3 face, resulting in a B(10)–Cu–P angle of 162.9 (1)°. The C_2B_9 cage is not unusual; the C–C bond length of 1.586 (9) Å falls into the range observed in metallacarboranes containing icosahedral MC_2B_9 cage geometry,[24] and the lower B_5 plane approaches planarity (±0.006 Å).

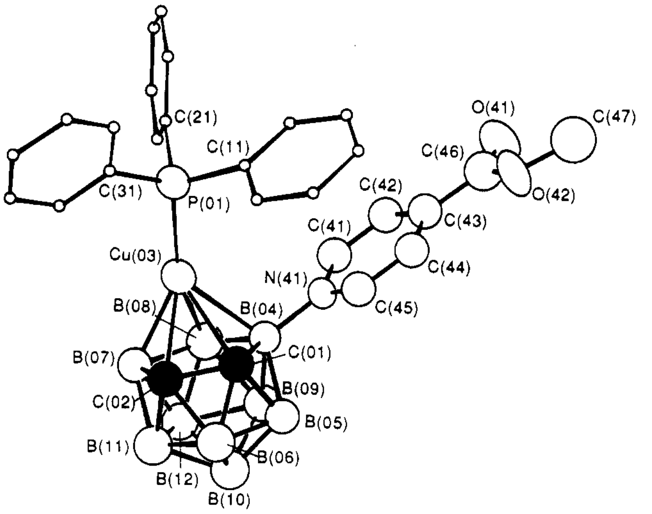

Figure 2. Molecular structure of [*closo*-3-(PPh_3)-4-(4-(C_5H_4N)-CO_2CH_3)-3,1,2-$CuC_2B_9H_{10}$] (**5**) showing the atom-labeling scheme. All hydrogen atoms have been omitted for clarity.

The structural changes in the MC_2B_9 cage geometry upon the replacement of a terminal hydride on boron by a Lewis base are not readily predictable. Complex **5**, a boron-substituted analogue of **3** with methyl isonicotinate as a substituent, is such an example. The molecular structure of **5**, as displayed in Figure 2, shows structural changes in accord with a similar trend observed in distorted η^3-borallylic type sandwich complexes.[6] Upon molecular distortion, the metal–carbon distances increase with a concomitant shortening in the carborane C–C bond. The values of the structural parameters for **5**, tabulated in Table II, support this view. As will be discussed below, compound **5** adopts an MC_2B_9 cage geometry intermediate between closo and nido. Thus, when the distances are compared to those in compound **3**, lengthening in Cu–C distances and shortening in C–C bond lengths result. Consequently, it is apparent that the methyl isonicotinate substituent is not electronically "innocent". Supporting this are the observations that the crystal structure of **5** does not reveal unusual crystal-packing features and the color of Na[**2**] in THF is deep bluish purple in contrast to the colorless solution of Na_2[**1**] in THF, indicative of a carborane anion-to-ligand charge-transfer excitation.[25] Unlike this active role played by the methyl isonicotinate substituent, the pyridine in [*closo*-3-(PPh_3)-3-CO-4-C_5H_5N-3,1,2-$RhC_2B_9H_{10}$] can be regarded as an innocent ligand both sterically and electronically.[12b]

---

(17) (a) Stone, F. G. A. *Acc. Chem. Res.* **1981**, *14*, 318. (b) Hoffmann, R. *Angew. Chem., Int. Ed. Engl.* **1982**, *21*, 711.

(18) Cotton, F. A.; Takats, J. *J. Am. Chem. Soc.* **1970**, *92*, 2353.

(19) Lippard, S. J.; Melmed, K. M. *Inorg. Chem.* **1967**, *6*, 2223.

(20) Lippard, S. J.; Melmed, K. M. *Inorg. Chem.* **1969**, *8*, 2755.

(21) Bartlett, N.; Palenik, G. J. *Acta Crystallogr., Sect. A: Cryst. Phys., Diffr., Theor. Gen. Crystallogr.* **1969**, *A25*, S173.

(22) Messmer, G. G.; Palenik, G. J. *Can. J. Chem.* **1969**, *47*, 1440.

(23) Gill, J. T.; Lippard, S. J. *Inorg. Chem.* **1975**, *14*, 751.

(24) Grimes, R. N. In *Comprehensive Organometallic Chemistry*; Wilkinson, G., Stone, F. G. A.; Abel, E. W.; Eds.; Pergamon: New York, 1982; Vol. 1, Chapter 5.

(25) Graybill, B. M.; Hawthorne, M. F. *J. Am. Chem. Soc.* **1961**, *83*, 2673.

Table II. Selected Interatomic Distances (Å) and Angles (deg) for [*closo*-3-(PPh_3)-4-(4-$(C_5H_4N)CO_2CH_3$)-3,1,2-$CuC_2B_9H_{10}$] (**5**)

Distances

Cu(03)–P(01)	2.163 (3)	Cu(03)–C(01)	2.480 (9)
Cu(03)–C(02)	2.383 (9)	Cu(03)–B(04)	2.254 (10)
Cu(03)–B(07)	2.150 (12)	Cu(03)–B(08)	2.116 (11)
P(01)–C(11)	1.823 (7)	P(01)–C(21)	1.820 (8)
P(01)–C(31)	1.822 (9)	O(41)–C(46)	1.196 (13)
O(42)–C(46)	1.326 (12)	O(42)–C(47)	1.445 (13)
N(41)–C(41)	1.353 (10)	N(41)–C(45)	1.327 (11)
N(41)–B(04)	1.538 (12)	C(41)–C(42)	1.360 (13)
C(42)–C(43)	1.373 (12)	C(43)–C(44)	1.406 (12)
C(43)–C(46)	1.505 (14)	C(44)–C(45)	1.381 (13)
C(01)–C(02)	1.562 (13)	C(01)–B(04)	1.653 (13)
C(01)–B(05)	1.707 (14)	C(01)–B(06)	1.708 (15)
C(02)–B(06)	1.725 (15)	C(02)–B(07)	1.696 (14)
C(02)–B(11)	1.704 (16)	B(04)–B(05)	1.799 (15)
B(04)–B(08)	1.781 (15)	B(04)–B(09)	1.763 (16)
B(05)–B(06)	1.763 (17)	B(05)–B(09)	1.761 (16)
B(05)–B(10)	1.760 (20)	B(06)–B(10)	1.770 (20)
B(06)–B(11)	1.750 (20)	B(07)–B(08)	1.835 (16)
B(07)–B(11)	1.840 (20)	B(07)–B(12)	1.818 (16)
B(08)–B(09)	1.775 (16)	B(08)–B(12)	1.772 (17)
B(09)–B(10)	1.810 (20)	B(09)–B(12)	1.789 (17)
B(10)–B(11)	1.790 (20)	B(10)–B(12)	1.810 (20)
B(11)–B(12)	1.753 (17)		

Angles

P(01)–Cu(03)–C(01)	120.8 (2)	P(01)–Cu(03)–C(02)	130.4 (2)
P(01)–Cu(03)–B(04)	127.7 (3)	P(01)–Cu(03)–B(07)	150.4 (3)
P(01)–Cu(03)–B(08)	153.3 (3)	C(01)–Cu(03)–C(02)	37.4 (3)
C(01)–Cu(03)–B(04)	40.5 (3)	C(01)–Cu(03)–B(07)	72.4 (4)
C(01)–Cu(03)–B(08)	74.2 (4)	C(02)–Cu(03)–B(04)	69.2 (3)
C(02)–Cu(03)–B(07)	43.6 (4)	C(02)–Cu(03)–B(08)	75.4 (4)
B(04)–Cu(03)–B(07)	80.3 (4)	B(04)–Cu(03)–B(08)	48.0 (4)
B(07)–Cu(03)–B(08)	51.0 (4)	Cu(03)–P(01)–C(11)	110.7 (2)
Cu(03)–P(01)–C(21)	112.9 (3)	Cu(03)–P(01)–C(31)	116.6 (3)
C(11)–P(01)–C(21)	105.8 (3)	C(11)–P(01)–C(31)	104.8 (3)
C(21)–P(01)–C(31)	105.2 (3)	C(41)–N(41)–C(45)	117.7 (7)
C(41)–N(41)–B(04)	120.9 (7)	C(45)–N(41)–B(04)	121.3 (7)
N(41)–C(41)–C(42)	123.0 (8)	C(41)–C(42)–C(43)	119.3 (8)
C(42)–C(43)–C(44)	118.9 (8)	C(42)–C(43)–C(46)	119.7 (8)
C(44)–C(43)–C(46)	121.3 (8)	C(43)–C(44)–C(45	117.7 (8)
N(41)–C(45)–C(44)	123.4 (8)	C(43)–C(46)–O(41)	124.3 (9)
C(43)–C(46)–O(42)	110.2 (8)	O(41)–C(46)–O(42)	125.5 (9)
C(46)–O(42)–C(47)	116.4 (8)	C(02)–C(01)–B(04)	109.9 (7)
C(01)–C(02)–B(07)	114.9 (7)	Cu(03)–B(04)–N(41)	107.9 (6)
N(41)–B(04)–C(01)	119.4 (7)	N(41)–B(04)–B(05)	112.9 (7)
N(41)–B(04)–B(08)	127.6 (8)	N(41)–B(04)–B(09)	120.7 (7)
C(01)–B(04)–B(08)	108.4 (7)	B(06)–B(05)–B(09)	108.8 (8)
B(05)–B(06)–B(11)	107.6 (8)	C(02)–B(07)–B(08)	102.7 (7)
B(04)–B(08)–B(07)	103.6 (7)	B(05)–B(09)–B(12)	107.0 (8)
B(06)–B(11)–B(12)	108.8 (9)	B(09)–B(12)–B(11)	107.8 (8)
P(01)–Cu(03)–B(10)	159.1 (2)		

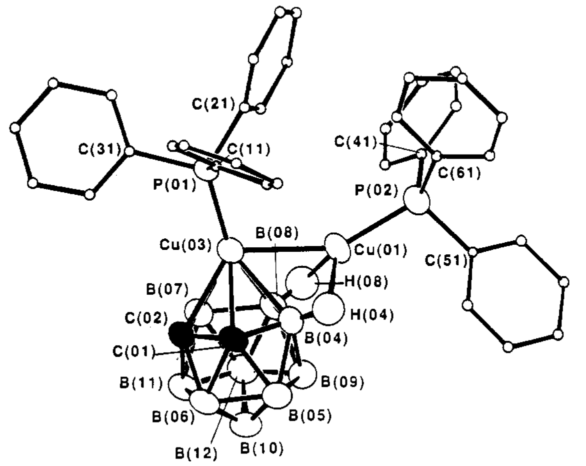

Figure 3. Molecular structure of [*closo-exo*-4,8-{$(\mu$-H$)_2$Cu(PPh_3)}-3-(PPh_3)-3,1,2-$CuC_2B_9H_9$] (**4**) showing the atom-labeling scheme. All hydrogen atoms except the bridging hydrides have been omitted for clarity.

Table III. Selected Interatomic Distances (Å) and Angles (deg) for [*closo-exo*-4,8-{$(\mu$-H$)_2$Cu(PPh_3)}-3-(PPh_3)-3,1,2-$CuC_2B_9H_9$] (**4**)

Distances

Cu(01)–Cu(03)	2.576 (1)	Cu(01)–P(02)	2.197 (1)
Cu(01)–B(04)	2.173 (5)	Cu(01)–B(08)	2.210 (4)
Cu(03)–P(01)	2.164 (1)	Cu(03)–C(01)	2.331 (4)
Cu(03)–C(02)	2.280 (4)	Cu(03)–B(04)	2.226 (5)
Cu(03)–B(07)	2.164 (5)	Cu(03)–B(08)	2.140 (5)
P(01)–C(11)	1.817 (3)	P(01)–C(21)	1.814 (2)
P(01)–C(31)	1.826 (3)	P(02)–C(41)	1.812 (3)
P(02)–C(51)	1.822 (3)	P(02)–C(61)	1.806 (3)
Cu(01)–H(04)	2.03 (4)	Cu(01)–H(08)	1.91 (4)
C(01)–C(02)	1.573 (6)	C(01)–B(04)	1.634 (6)
C(01)–B(05)	1.727 (6)	C(01)–B(06)	1.714 (6)
C(02)–B(06)	1.732 (6)	C(02)–B(07)	1.672 (7)
C(02)–B(11)	1.705 (6)	B(04)–B(05)	1.785 (7)
B(04)–B(08)	1.814 (6)	B(04)–B(09)	1.797 (7)
B(05)–B(06)	1.752 (7)	B(05)–B(09)	1.775 (7)
B(05)–B(10)	1.753 (8)	B(06)–B(10)	1.768 (8)
B(06)–B(11)	1.778 (8)	B(07)–B(08)	1.785 (7)
B(07)–B(11)	1.784 (7)	B(07)–B(12)	1.793 (7)
B(08)–B(09)	1.798 (7)	B(08)–B(12)	1.777 (6)
B(09)–B(10)	1.784 (7)	B(09)–B(12)	1.787 (7)
B(10)–B(11)	1.769 (7)	B(10)–B(12)	1.783 (7)
B(11)–B(12)	1.762 (7)	B(04)–H(04)	1.08 (4)
B(08)–H(08)	1.06 (4)		

Angles

Cu(03)–Cu(01)–P(02)	150.6 (1)	Cu(03)–Cu(01)–B(04)	55.1 (1)
Cu(03)–Cu(01)–B(08)	52.4 (1)	P(02)–Cu(01)–B(04)	146.8 (1)
P(02)–Cu(01)–B(08)	150.7 (1)	B(04)–Cu(01)–B(08)	48.9 (2)
Cu(01)–Cu(03)–P(01)	108.8 (1)	Cu(01)–Cu(03)–C(01)	94.5 (1)
Cu(01)–Cu(03)–C(02)	122.2 (1)	Cu(01)–Cu(03)–B(04)	53.2 (1)
Cu(01)–Cu(03)–B(07)	103.7 (1)	Cu(01)–Cu(03)–B(08)	54.9 (1)
P(01)–Cu(03)–C(01)	125.9 (1)	P(01)–Cu(03)–C(02)	125.9 (1)
P(01)–Cu(03)–B(04)	139.5 (1)	P(01)–Cu(03)–B(07)	139.1 (1)
P(01)–Cu(03)–B(08)	156.0 (1)	C(01)–Cu(03)–C(02)	39.9 (1)
C(01)–Cu(03)–B(04)	41.9 (2)	C(01)–Cu(03)–B(07)	74.0 (2)
C(01)–Cu(03)–B(08)	76.1 (2)	C(02)–Cu(03)–B(04)	72.2 (2)
C(02)–Cu(03)–B(07)	44.1 (2)	C(02)–Cu(03)–B(08)	76.5 (2)
B(04)–Cu(03)–B(07)	80.4 (2)	B(04)–Cu(03)–B(08)	49.0 (2)
B(07)–Cu(03)–B(08)	49.0 (2)	Cu(03)–P(01)–C(11)	114.0 (1)
Cu(03)–P(01)–C(21)	114.5 (1)	Cu(03)–P(01)–C(31)	113.9 (1)
C(11)–P(01)C(21)	104.3 (1)	C(11)–P(01)–C(31)	105.2 (1)
C(21)–P(01)–C(31)	103.7 (1)	Cu(01)–P(02)–C(41)	113.7 (1)
Cu(01)–P(02)–C(51)	109.0 (1)	Cu(01)–P(02)–C(61)	118.3 (1)
C(41)–P(02)–C(51)	106.9 (1)	C(41)–P(02)–C(61)	103.0 (1)
C(51)–P(02)–C(61)	105.1 (1)	Cu(01)–H(04)–B(04)	83 (2)
Cu(01)–H(08)–B(08)	92 (2)	C(02)–C(01)–B(04)	111.7 (3)
C(01)–C(02)–B(07)	113.2 (3)	C(01)–B(04)–B(08)	106.3 (3)
B(06)–B(05)–B(09)	109.1 (3)	B(05)–B(06)–B(11)	107.4 (3)
C(02)–B(07)–B(08)	104.8 (3)	B(04)–B(08)–B(07)	104.0 (3)
B(05)–B(09)–B(12)	107.2 (3)	B(06)–B(11)–B(12)	108.7 (4)
B(09)–B(12)–B(11)	107.6 (3)	P(01)–Cu(03)–B(10)	162.5 (1)

(b) Dinuclear Complex 4. The crystal structure of **4** consists of two enantiomers related by an inversion center to form a racemic system. The structure of **4**, shown in Figure 3, contains one dianionic $C_2B_9H_{11}$ cage and two cationic $[(PPh_3)Cu^I]$ moieties. In a formal sense, the neutral compound **4** is a zwitterion composed of an anionic **3**, $[(PPh_3)CuC_2B_9H_{11}]^-$, complexed with a $[Cu(PPh_3)]^+$ cation. The interatomic distance between the two formal d^{10}-Cu(I) centers is 2.576 (1) Å. Other selected structural parameters are listed in Table III. The two copper centers are bonded to one C_2B_9 cage via the open pentagonal C_2B_3 face and two exopolyhedral boron–hydride–metal three-center–two-electron linkages as in mode I. Bridging unit I is not uncommon in metallaboranes[23,26] or mononuclear metallacarboranes.[11c] In polynuclear dicarbollide metallacarboranes, the bridge bonding mode II is the most usual pattern encountered,[5,27–29] and prior to **4** the bonding mode I has only been realized in the bimetallic

I

II

---

[26] Kaesz, H. D.; Fellman, W.; Wilkes, G. R.; Dahl, L. F. *J. Am. Chem. Soc.* **1965**, *87*, 2753.

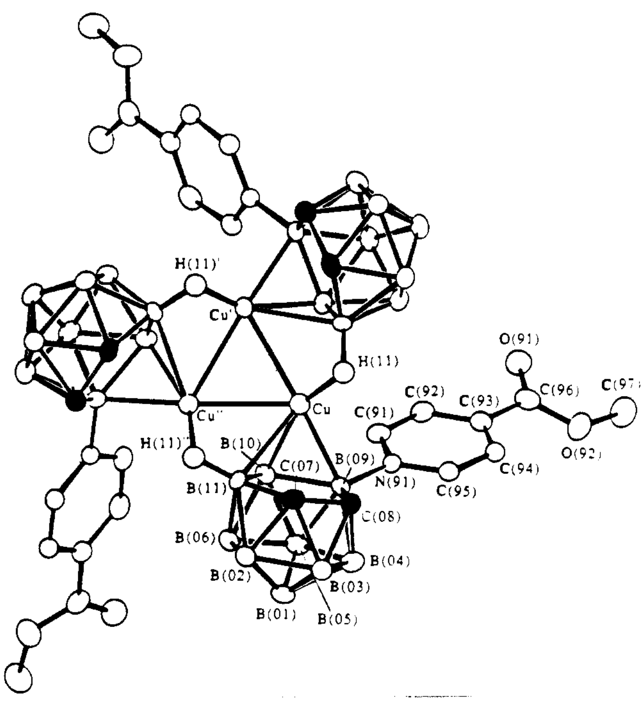

Figure 4. Molecular structure of $[Cu_3(\mu\text{-}H)_3\{C_2B_9H_9(4\text{-}(C_5H_4N)CO_2CH_3)\}_3]$ (**6**) showing the atom-labeling scheme. All hydrogen atoms except the bridging hydrides have been omitted for clarity.

Table IV. Selected Interatomic Distances (Å) and Angles (deg) for $[Cu_3(\mu\text{-}H)_3\{C_2B_9H_9(4\text{-}(C_5H_4N)CO_2CH_3)\}_3]\cdot n\text{-}C_7H_{16}$ (**6**$\cdot n\text{-}C_7H_{16}$)[a]

	Distances		
Cu–Cu′	2.519 (2)	Cu–H(11)	1.608
Cu–C(07)	2.634 (9)	Cu–C(08)	2.635 (9)
Cu–B(09)	2.265 (8)	Cu–B(10)	2.116 (8)
Cu–B(11)	2.307 (8)	Cu″–B(11)	2.120 (8)
O(91)–C(96)	1.196 (9)	O(92)–C(96)	1.330 (9)
O(92)–C(97)	1.447 (9)	N(91)–C(91)	1.356 (9)
N(91)–C(95)	1.343 (9)	N(91)–B(09)	1.552 (9)
C(91)–C(92)	1.379 (10)	C(92)–C(93)	1.382 (11)
C(93)–C(94)	1.390 (10)	C(93)–C(96)	1.499 (10)
C(94)–C(95)	1.372 (10)	C(07)–C(08)	1.553 (10)
C(07)–B(02)	1.722 (11)	C(07)–B(03)	1.727 (11)
C(07)–B(11)	1.641 (11)	C(08)–B(03)	1.725 (11)
C(08)–B(04)	1.713 (11)	C(08)–B(09)	1.662 (10)
B(01)–B(02)	1.764 (12)	B(01)–B(03)	1.771 (12)
B(01)–B(04)	1.761 (12)	B(01)–B(05)	1.796 (12)
B(01)–B(06)	1.787 (12)	B(02)–B(03)	1.770 (12)
B(02)–B(06)	1.786 (12)	B(02)–B(11)	1.806 (11)
B(03)–B(04)	1.766 (12)	B(04)–B(05)	1.766 (12)
B(04)–B(09)	1.809 (11)	B(05)–B(06)	1.793 (12)
B(05)–B(09)	1.772 (11)	B(05)–B(10)	1.791 (12)
B(06)–B(10)	1.795 (12)	B(06)–B(11)	1.810 (12)
B(09)–B(10)	1.759 (11)	B(10)–B(11)	1.821 (11)
B(11)–H(11)″	1.214		
	Angles		
Cu–Cu′–Cu″	60	Cu′–Cu–H(11)	85.8
Cu′–Cu–B(09)	156.3 (2)	Cu′–Cu–B(10)	117.4 (2)
Cu′–Cu–B(11)	109.9 (2)	Cu′–Cu–B(11)′	58.9 (2)
Cu″–Cu–B(09)	114.0 (2)	Cu″–Cu–(10)	67.9 (2)
Cu″–Cu–B(11)	51.9 (2)	Cu″–Cu–B(11)′	116.7 (2)
Cu″–Cu–H(11)	128.0	H(11)–Cu–B(09)	111.8
H(11)–Cu–B(10)	156.6	H(11)–Cu–B(11)	123.7
B(09)–Cu–B(10)	47.2 (3)	B(09)–Cu–B(11)	74.3 (3)
B(09)–Cu–B(11)′	128.6 (3)	B(10)–Cu–B(11)	48.4 (3)
B(10)–Cu–B(11)′	162.0 (3)	B(11)–Cu–B(11)′	148.9 (4)
C(91)–N(91)–C(95)	119.4 (6)	C(91)–N(91)–B(09)	117.9 (6)
C(95)–N(91)–B(09)	122.7 (6)	N(91)–C(91)–C(92)	121.4 (7)
C(91)–C(92)–C(93)	118.9 (7)	C(92)–C(93)–C(94)	119.5 (7)
C(92)–C(93)–C(96)	117.6 (7)	C(94)–C(93)–C(96)	122.9 (7)
C(93)–C(94)–C(95)	118.9 (7)	N(91)–C(95)–C(94)	121.9 (7)
C(93)–C(96)–O(91)	123.4 (7)	C(93)–C(96)–O(92)	112.9 (7)
O(91)–C(96)–O(92)	123.7 (7)	C(96)–O(92)–C(97)	115.0 (6)
C(08)–C(07)–B(11)	112.8 (5)	C(07)–C(08)–B(09)	110.1 (6)
B(03)–B(02)–B(06)	108.6 (6)	B(02)–B(03)–B(04)	107.2 (6)
B(03)–B(04)–B(05)	109.7 (6)	B(04)–B(05)–B(06)	107.1 (6)
B(02)–B(06)–B(05)	107.4 (6)	Cu–B(09)–N(91)	104.7 (4)
Cu–B(09)–C(08)	82.8 (4)	N(91)–B(09)–C(08)	120.0 (6)
N(91)–B(09)–B(04)	111.2 (6)	N(91)–B(09)–B(05)	118.0 (6)
N(91)–B(09)–B(10)	127.1 (6)	C(08)–B(09)–B(10)	109.2 (6)
B(09)–B(10)–B(11)	100.9 (5)	Cu–B(11)–Cu″	69.2 (2)
Cu–B(11)–C(07)	81.9 (4)	Cu–B(11)–H(11)″	105.9
Cu″–B(11)–C(07)	140.1 (6)	Cu″–B(11)–B(02)	154.9 (5)
Cu″–B(11)–B(06)	113.0 (5)	Cu″–B(11)–B(10)	82.5 (4)
Cu″–B(11)–H(11)″	48.9	C(07)–B(11)–B(10)	106.8 (6)
C(07)–B(11)–H(11)″	120.1	H(11)″–B(11)–B(02)	111.6
H(11)″–B(11)–B(06)	120.3	H(11)″–B(11)–B(10)	129.0
Cu–H(11)–B(11)′	96.4		

[a] Positions marked with a single prime correspond to $-y, x - y, z$, and positions marked with a double prime correspond to $y - x, -x, z$.

aluminacarborane *commo*-3,3′-Al[(*exo*-8,9-$(\mu\text{-}H)_2Al(C_2H_5)_2$-3,1,2-$AlC_2B_9H_9$)(3′,1′,2′-$AlC_2B_9H_{11}$)],[30] in which the bridging BH units originate from the upper and lower pentagonal belts of one dicarbollide cage. In compound **4**, both bridging BH units stem from the upper pentagonal belt of the cage such that the pentagonal C_2B_3 plane (±0.016 Å) forms a dihedral angle of 40.9° with the plane of Cu(01)–B(04)–B(08) and close proximity of two copper(I) centers results. The mean exo Cu–(μ-H) distance of 1.97 (4) Å falls into the range (~1.70–2.08 Å) observed in copper hydroborate complexes[10,31] and in $[Mo_2Cu_2(\mu\text{-}CO)_4(CO)_2(\mu\text{-}H)_2(C_2B_9H_{10})_2]^{2-}$.[5]

(c) Trinuclear Complex 6·*n*-C_7H_{16}. The crystal structure of the racemic system consists of well-separated neutral trinuclear cupracarborane clusters and disordered *n*-heptane solvate molecules. Since single-crystal X-ray analysis performed at 298 K revealed a severely disordered solvate molecule, a low-temperature X-ray diffraction study has been carried out. The structure of one enantiomeric form of **6** is illustrated in Figure 4. The trinuclear cupracarborane **6** contains three $[CuC_2B_9H_{10}(4\text{-}(C_5H_4N)CO_2CH_3)]$ units, which are linked by both Cu–H–B and Cu–Cu interactions about a crystallographic 3-fold axis such that a "pinwheel" ligand array around an equilateral Cu_3 core results. This pinwheel array can be further described by considering the three equilateral triangles Cu_3, H_3, and B_3 associated with the three Cu–H–B bridge bonds. The three planes of Cu_3, B_3, and H_3 triangles are parallel to each other with interplanar distances of 0.549 Å between the Cu_3 and the B_3 plane and 0.501 Å between the B_3 and H_3 plane.

The triangular Cu_3 geometry in **6** is found often in trinuclear complexes but constitutes the first example of a discrete equilateral metallic core of copper(I) atoms with a relatively short copper–copper distance of 2.519 (2) Å. Several trinuclear complexes containing scalene[32] or isosceles[33] Cu_3 triangles, whose edge distances range from ca. 2.750 to 3.610 Å, have been previously reported. The triangular Cu_3 core has also been observed in a heteropolynuclear raft system[34] as well as in polymeric copper

---

(27) Green, M.; Howard, J. A. K.; James, A. P.; Jelfs, A. N. de M.; Nunn, C. M.; Stone, F. G. A. *J. Chem. Soc., Chem. Commun.* **1985**, 1778.

(28) Baker, R. T.; King, R. E., III; Knobler, C. B.; O'Con, C. A.; Hawthorne, M. F. *J. Am. Chem. Soc.* **1978**, *100*, 8266.

(29) Behnken, P. E.; Marder, T. B.; Baker, R. T.; Knobler, C. B.; Thompson, M. R.; Hawthorne, M. F. *J. Am. Chem. Soc.* **1985**, *107*, 932.

(30) Rees, W. S., Jr.; Schubert, D. M.; Knobler, C. B.; Hawthorne, M. F. *J. Am. Chem. Soc.* **1986**, *108*, 5367.

(31) Teller, R. G.; Bau, R. *Struct. Bonding (Berlin)* **1981**, *44*, 1.

(32) (a) Rao, Ch. P.; Dorfman, J. R.; Holm, R. H. *Inorg. Chem.* **1986**, *25*, 428. (b) Ho, D. M.; Bau, R. *Inorg. Chem.* **1983**, *22*, 4079. (c) Nardin, G.; Randaccio, L.; Zangrando, E. *J. Chem. Soc., Dalton Trans.* **1975**, 2566. (d) Camus, A.; Marsich, N.; Nardin, G.; Randaccio, L. *J. Organomet. Chem.* **1973**, *60*, C39.

(33) (a) Bresciani, N.; Marsich, N.; Nardin, G.; Randaccio, L. *Inorg. Chim. Acta* **1974**, *10*, L5. (b) Tiethof, J. A.; Stalick, J. K.; Corfield, P. W. R.; Meek, D. W. *J. Chem. Soc., Chem. Commun.* **1972**, 1141.

(34) (a) Lemmen, T. H.; Huffman, J. C.; Caulton, K. G. *Angew. Chem., Int. Ed. Engl.* **1986**, *25*, 262. (b) Doyle, G.; Eriksen, K. A.; Van Engen, D. *J. Am. Chem. Soc.* **1986**, *108*, 445. (c) Doyle, G.; Eriksen, K. A.; Van Engen, D. *J. Am. Chem. Soc.* **1985**, *107*, 7914.

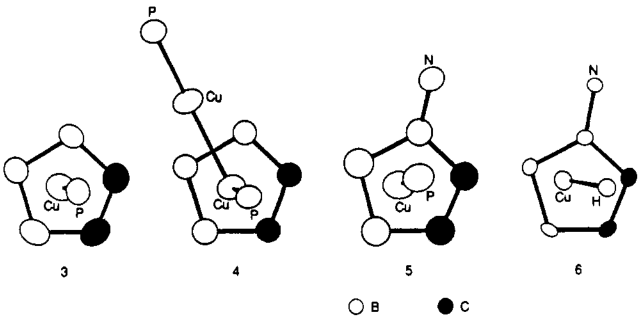

Figure 5. Projections of the copper atom and upper belt atoms (3 B and 2 C) on the plane defined by five boron atoms in the lower belt of the C_2B_9 cage, showing the slippage of the copper atom.

complex systems.[35] The Cu_3 plane forms dihedral angles of 79.5 and 80.4° with the upper C_2B_3 plane (±0.024 Å) and the lower B_5 plane (±0.001 Å) of the cage, respectively.

In Table IV, selected interatomic distances and angles for **6** are listed. The values of the Cu–(μ-H) bond (1.608 Å) and the Cu–(μ-H)–B angle (96.4°) for the bridging mode II observed in compound **6** are similar to those (1.69 (6) Å and 97 (3)°) for the bridging Cu–H–B interaction found in the tetranuclear metallacarborane $[Mo_2Cu_2(\mu\text{-}CO)_4(CO)_2(\mu\text{-}H)_2(C_2B_9H_{10})_2]^{2-}$.[5] The dicarbollide carbon–carbon distance of 1.553 (10) Å in **6** is the shortest among the four cupracarboranes discussed in this paper.

The experimental observation that the attempted preparation of $[Cu_3(\mu\text{-}H)_3(C_2B_9H_{10})_3]^{3-}$, a trinuclear analogue of **6** with the dianionic dicarbollide anion **1**, was not successful due to an undesirable redox reaction implies that the methyl isonicotinate substituent interacts electronically with the C_2B_9 cage as in compound **5** and supports the formation and stabilization of a triangular d^{10}-Cu_3 core in **6**. The nicotinate ring is not parallel to the C_2B_3 plane and forms a dihedral angle of 21.6°. Finally, the methyl isonicotinate substituent ring does not seem to impose any structural effect arising from crystal packing.

(d) Geometry of the Polyhedral Framework of the CuC_2B_9 Fragment in 3–6. The polyhedral CuC_2B_9 unit is the common structural feature displayed by all four cupracarboranes. Structural studies on metallacarboranes derived from the nido anion **1** have revealed two fundamental geometries for the MC_2B_9 cage, the symmetrically bonded closo structure adopted by d^n ($n \leq 7$) transition-metal ions and the distorted nido or slipped geometry observed for complexes containing formal d^n (n = 8–10) metal ions.[24] For electron-rich late- and post-transition-element metallacarboranes derived from ligand **1**, a progressive decrease in the extent of metal–cage bonding occurs as the number of electrons associated with the metal increases.[7b,e] The isoelectronic 18-electron series of $[Re(CO)_3C_2B_9H_{11}]^-$ (d^6, Re^I),[36] $[Au(S_2CNEt_2)C_2B_9H_{11}]$ (d^8, Au^{III}),[7a,c] $[Hg(PPh_3)C_2B_9H_{11}]$ (d^{10}, Hg^{II}),[7b,e] and $[TlC_2B_9H_{11}]^-$ (d^{10} s^2, Tl^I)[7b,37] illustrates the progressive opening of the MC_2B_9 cage as a trend in the structural changes. This progressive cage opening has been explained in a molecular orbital sense,[8] but terms of molecular distortions such as the slipping,[6,8] folding,[8] and tilting[7c,e] distortions remain useful for the description of the MC_2B_9 cage.

The structural analysis of **3**–**6** reveals the unusual feature that opening of the (d^{10}-Cu)C_2B_9 icosahedra increases in the order of **3**, **4**, **5**, and **6**, resulting in closo geometry for **3** and **4**, nido geometry for **6**, and intermediate geometry for **5**. In all four compounds, the lower B_5 planes are nearly planar while the upper C_2B_3 planes experience distortion whose extent can be described in terms of the folding parameters θ and ϕ.[8] Figure 5, a set of projections of the copper atom and upper C_2B_3 belt atoms onto the lower B_5 plane of the C_2B_9 cage, pictures the displacement of the copper atom from the perpendicular passing through the centroid of the lower B_5 plane, known as the slipping parameter Δ.[5] Table V lists values for these distortion parameters as well as other measures, including ratios of mean Cu–C/Cu–B distances, related to the CuC_2B_9 cage distortion. The previously observed ranges for $\theta + \phi$, Δ, and Cu–C/Cu–B ratio are 3.6–9.7°, 0.05–0.26 Å, and 0.97–1.08 for the closo icosahedral non-commo metallacarborane systems[38] and 9.1–17.2°, 0.42–0.52 Å, and 1.13–1.26 for the slipped icosahedral non-commo metallacarboranes,[7a,c,d,8] respectively. The values for the distortion parameters of the compounds **3** and **4** fall into the range observed in metallacarboranes with closo MC_2B_9 geometry. Similar structural comparison indicates that compound **5** adopts a CuC_2B_9 geometry intermediate between closo and nido while the structure of **6** contains nido geometry, resulting in η^3-borallylic ligation of C_2B_9 cages to the copper atoms. Compounds **3** and **4** constitute the first examples of structurally characterized d^{10}-element metallacarboranes with closo MC_2B_9 geometry. The methyl isonicotinate substituent in **5** and **6** is not electronically innocent and encourages cage opening in this cupracarborane series.

Table V. Parameters Related to the CuC_2B_9 Cage Distortion

	3	4	5	6
dist, Å				
Cu–C_2B_3 plane	1.678	1.688	1.720	1.844
mean Cu–C(C_2B_3)	2.317	2.306	2.432	2.635
mean Cu–B(C_2B_3)	2.155	2.177	2.173	2.229
C–C(C_2B_3)	1.586 (9)	1.573 (6)	1.562 (13)	1.553 (10)
θ (C_2B_2/B_5), deg	2.4	2.3	3.2	1.6
ϕ (B_3/B_5), deg	1.6	1.1	3.5	2.0
Δ, Å	0.211	0.248	0.409	0.594
Cu–C/Cu–B	1.07	1.06	1.12	1.18

(e) Extent of Cu(I)–Cu(I) Interaction in 4 and 6. In polynuclear copper(I) compounds, a range of Cu(I)–Cu(I) distances from 2.35 to about 3.61 Å is found.[33,34,39] The short distances might be considered to imply the existence of copper–copper interactions but might also result from ligand stereochemical requirements, since in each case there are ligand bridges. MO calculations made for several representative systems suggest that direct copper(I)–copper(I) interactions are at best weak, and possibly negligible.[39b,40] The bridging ligand stereochemistry, which dominates, for example, in $[Cu_2(tmen)_2(\mu\text{-}CO)(\mu\text{-}PhCO_2)]^+$, resulting in the very short Cu(I)–Cu(I) distance of 2.419 (2) Å,[39c] is likely to be minimal in **4** since the elevation angles of the hydrogen substituents in the $CuC_2B_9H_{11}$ cage are not restricted to that (26°) of a regular icosahedron.[8b] Thus the relatively close approach (2.576 (1) Å) of the 18-electron copper(I) center and the 16-electron copper(I) center in **4** can be considered to be a consequence of a Cu(I)–Cu(I) interaction similar to the Fe–Fe interaction found in $Fe_2(CO)_6C_4(CH_3)_2(OH)_2$[41] and its homologues.[42] In the trinuclear cupracarborane **6**, the interatomic Cu(I)–Cu(I) separations of 2.519 (2) Å, which is shorter than the Cu–Cu distances of 2.56 Å found in Cu metal,[43] can also be described in terms of a metal–metal interaction since the requirements of the bridging ligand seem to be even less than in **4**.

---

(35) Hartl, H.; Mahdjour-Hassan-Abadi, F. *Z. Naturforsch, B: Anorg. Chem., Org. Chem.* **1984**, *39B*, 149.

(36) Zalkin, A.; Hopkins, T. E.; Templeton, D. H. *Inorg. Chem.* **1966**, *5*, 1189.

(37) Colquhoun, H. M.; Greenhough, T. J.; Wallbridge, M. G. H. *Acta Crystallogr., Sect. B: Struct. Crystallogr. Cryst. Chem.* **1978**, *B34*, 2373.

(38) () See ref 7d, 12b, 28, 29, and 36. (b) Walker, J. A.; Knobler, C. B.; Hawthorne, M. F. *Inorg. Chem.* **1985**, *24*, 2688. (c) Zheng, L.; Baker, R. T.; Knobler, C. B.; Walker, J. A.; Hawthorne, M. F. *Inorg. Chem.* **1983**, *22*, 3350. (d) Kalb, W. C.; Teller, R. G.; Hawthorne, M. F. *J. Am. Chem. Soc.* **1979**, *101*, 5417. (e) Demidowicz, Z.; Teller, R. G.; Hawthorne, M. F. *J. Chem. Soc., Chem. Commun.* **1979**, 831. (f) Hardy, G. E.; Callahan, K. P.; Strouse, C. E.; Hawthorne, M. F. *Acta Crystallogr., Sect. B: Struct. Crystallogr. Cryst. Chem.* **1976**, *B32*, 264.

(39) (a) Reference 4 and references cited therein. (b) Mehrotra, P. K.; Hoffmann, R. *Inorg. Chem.* **1978**, *17*, 2187 and references cited therein. (c) Pasquali, M.; Floriani, C.; Gaetani-Manfredotti, A.; Guastini, C. *J. Am. Chem. Soc.* **1981**, *103*, 185.

(40) Avdeef, A.; Fackler, J. P., Jr. *Inorg. Chem.* **1978**, *17*, 2182.

(41) Hock, A. A.; Mills, O. S. *Acta Crystallogr.* **1961**, *14*, 139.

(42) (a) Chin, H. B.; Bau, R. *J. Am. Chem. Soc.* **1973**, *95*, 5068. (b) Dettlaf, G.; Weiss, E. *J. Organomet. Chem.* **1976**, *108*, 213.

(43) Wells, A. F. *Structural Inorganic Chemistry*, 5th ed.; Oxford University Press: Oxford, England, 1984; p 1104.

Scheme II

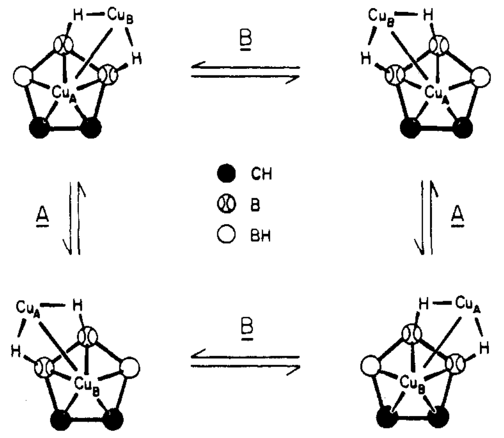

Dynamic Processes. Since the metal vertex of 12-vertex *closo*-phosphinometallacarboranes undergoes hindered rotation with respect to the five-membered C_2B_3 face of the carborane cage in the solution phase,[44] similar processes might be operative in solution for the mononuclear 12-vertex *closo*-phosphinocupracarboranes **3** and **5**. Although the existence of this dynamic process involving the copper vertex remains speculative, the methyl isonicotinate groups in compounds **5** and **6** exhibit unhindered rotation in solution as low as 198 K as observed by variable-temperature ^1H FT NMR spectroscopy. The cupracarborane **4**, whose dinuclear structural integrity remains intact upon dissolution, displays an interesting sort of fluxionality. The molecular structure of **4** (Figure 3) indicates the presence of two distinguishable phosphorus atoms, but in solution the two phosphorus nuclei become inequivalent only below 253 K. The variable-temperature 81.02-MHz $^{31}P\{^1H\}$ FT NMR spectra of **4** in dichloromethane, as displayed in Figure 6, clearly show that coalescence occurs at 253 K and below this temperature a fluxional process involving both phosphorus nuclei becomes inoperative. However, the two CH hydrogens of the carborane cage remain indistinguishable in ^1H FT NMR spectra even at 203 K, indicating that at least one kind of dynamic process is still present at this temperature. The evidence at hand does not unequivocally reveal the nature of the dynamic processes but leads to two possible fluxional pathways as shown in Scheme II. The exchange process A involves both closo and exo copper atoms and makes the two phosphorus nuclei indistinguishable above the coalescence temperature. The free energy of activation $\Delta G^{\ddagger}$ for the exchange process A was calculated as 11.3 kcal/mol by means of the Eyring equation and the expression for the rate constant $k = \pi(\Delta\nu)/2^{1/2}$, where $\Delta\nu$ is the chemical shift difference in hertz.[45] The indistinguishability of the two CH hydrogens as low as 203 K can be attributed to the wigwag process B, which involves an exo copper atom only and can be viewed as an extreme case of a hindered metal–cage rotation previously observed in *closo*-phosphinometallacarboranes.[44]

Experimental Section

Preparation of Compounds. All reactions were carried out under a pure dinitrogen or argon atmosphere. Solvents were carefully dried over an appropriate drying agent and degassed prior to use. Anhydrous cuprous chloride (Cerac), sodium hydride (Aldrich), and bis(triphenylphosphoranylidene) ammonium chloride ((PPN)Cl, Aldrich) were purchased and used as received. Triphenylphosphine (Aldrich) was recrystallized from ethyl alcohol. $[Tl_2C_2B_9H_{11}]$[46] and [*nido*-9-(4-$(C_5H_4N)CO_2CH_3$)-7,8-$C_2B_9H_{11}$][12a] were prepared according to literature methods. Details of the preparation and related chemistry of the latter will be reported separately.[13]

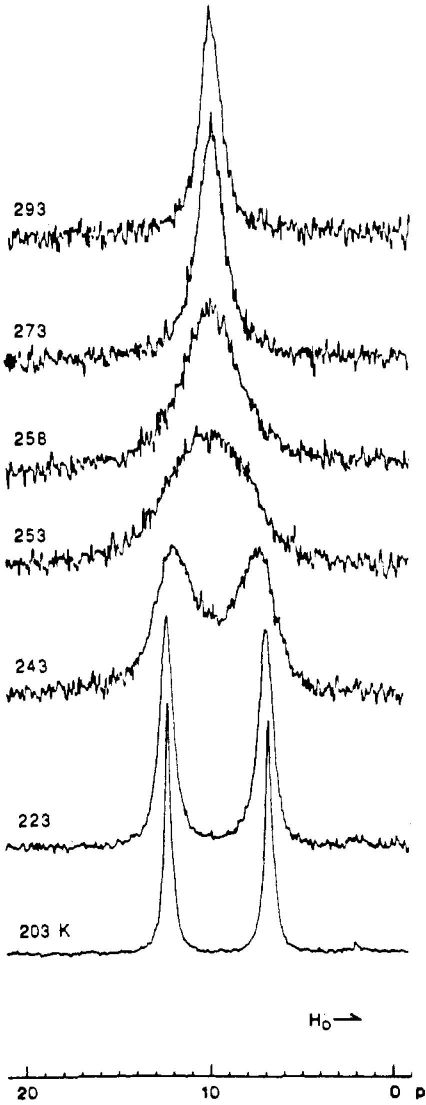

Figure 6. Variable-temperature 81.02-MHz $^{31}P\{^1H\}$ FT NMR spectra of complex **4** in 10% CD_2Cl_2/CH_2Cl_2.

PPN[*closo*-3-(PPh$_3$)-3,1,2-CuC$_2$B$_9$H$_{11}$] (PPN[3]). To a slurry of $[Tl_2C_2B_9H_{11}]$ (1 mmol) and (PPN)Cl (1 mmol) in 40 mL of CH_3CN was added a beige solution generated by stirring an equimolar slurry of anhydrous CuCl (1 mmol) and triphenylphosphine in 40 mL of CH_2Cl_2 for 1 h at 298 K. Stirring of the resulting white slurry for 20 h at 298 K was followed by removal of blue-gray solid by filtration. As the filtrate was reduced in volume, a slight blue tint became evident. The concentrated filtrate was treated with an excess amount of Et_2O. The resulting off-white crystals were collected, washed twice with Et_2O, dried in vacuo, and recrystallized from CH_2Cl_2/Et_2O, affording analytically pure product in a yield of 84% (845 mg). Anal. Calcd for $C_{56}H_{56}B_9P_3NCu$: C, 67.48; H, 5.56; B, 9.76; P, 9.92; N, 1.41; Cu, 6.37. Found: C, 67.44; H, 5.75; B, 9.57; P, 9.39; N, 1.36; Cu, 6.25. IR (cm^{-1}): 3052 (w), 2571 (w), 2537 (s), 2488 (s), 2418 (m), 1480 (w), 1436 (s), 1313 (s), 1300 (s), 1271 (m), 1115 (s), 1030 (w), 995 (w), 744 (m), 724 (s), 692 (s), 549 (s), 532 (s), 500 (s). ^1H NMR (ppm, CD_2Cl_2): 7.60–7.76 (envelope), 7.35–7.55 (envelope), 1.57 (s, carborane CH). $^{31}P\{^1H\}$ NMR (ppm, 10% CD_2Cl_2/CH_2Cl_2): 20.6 (PPN), 7.8 (PPh$_3$). $^{11}B\{^1H\}$ NMR (ppm, CH_2Cl_2): −17.2, −20.2, −22.1, −23.0, −24.9, −34.9.

[*closo*-*exo*-4,8-{(μ-H)$_2$Cu(PPh$_3$)}-3-(PPh$_3$)-3,1,2-CuC$_2$B$_9$H$_9$] (4). To a light beige solution generated by stirring an equimolar slurry of anhydrous CuCl (1 mmol) and triphenylphosphine in 40 mL of CH_2Cl_2 for 1 h at 298 K was added yellow solid $[Tl_2C_2B_9H_{11}]$ (0.5 mmol), resulting in the immediate disappearance of the yellow color and the formation of a white precipitate. After the resulting reaction mixture was stirred for 20 h at 298 K, blue-gray solid was removed by filtration through a Celite pad. The volume of colorless filtrate was reduced to 10 mL, and Et_2O was added to the concentrated filtrate, affording white crystalline solid, which was collected, washed twice with Et_2O, and dried in vacuo. Recrystallization from CH_2Cl_2/Et_2O afforded analytically pure product in a yield of 79% (315 mg). Anal. Calcd for $C_{38}H_{41}B_9P_2Cu_2$: C, 58.21;

---

(44) Marder, T. B.; Baker, R. T.; Long, J. A.; Doi, J. A.; Hawthorne, M. F. *J. Am. Chem. Soc.* **1981**, *103*, 2988.

(45) (a) Gutowsky, H. S.; Cheng, H. N. *J. Chem. Phys.* **1975**, *63*, 2439. (b) Kost, D.; Carlson, E. H.; Raban, M. *J. Chem. Soc., Chem. Commun.* **1971**, 656.

(46) Spencer, J. L.; Green, M.; Stone, F. G. A. *J. Chem. Soc., Chem. Commun.* **1972**, 1178.

Table VI. Details of Crystallographic Data Collections[a]

	PPN[**3**][b]	**4**[c]	**5**[d]	$\mathbf{6}\cdot{}^1/_3n\text{-}C_7H_{16}$[e]
M_r	997	784	594	835
temp, K	298	298	298	128
cryst size, mm	0.45 × 0.32 × 0.64	0.45 × 0.4 × 0.5	0.11 × 0.32 × 0.19	0.27 × 0.14 × 0.30
normal to face	010, 001, 100	010, 100, 001	010, 001, 120	012, 212, 112
appearance	colorless parallelepiped	colorless parallelepiped	orange parallelepiped	red platelet parallelepiped
space group	$P2_1/n$	$P2_1/n$	$P2_1/c$	$R\bar{3}$
a, Å	11.5070 (8)	10.005 (2)	13.798 (1)	17.280 (4)
b, Å	14.7717 (10)	20.693 (4)	12.072 (1)	
c, Å	30.7510 (20)	18.998 (3)	18.845 (2)	28.630 (7)
β, deg	90.284 (2)	92.664 (6)	95.111 (3)	
V, Å^3	5227	3924	3127	7457
Z	4	4	4	6
ρ(calcd), g cm^{-3}	1.27	1.33	1.26	1.34
μ, cm^{-1}	5.45	11.91	7.74	13.25
range of transmission factors	0.92–0.89, 0.91 (av)	0.81–0.77, 0.80 (av)	0.96–0.89, 0.95 (av)	0.92–0.86, 0.90 (av)
scan width below and above Kα_2, deg	1.3, 1.6	1.3, 1.6	1.3, 1.6	1.3, 1.6
scan rate, deg min^{-1}	6.0	3.0	4.5	6.0
no. of unique rflns	9219	6925	4078	3065
no. of obsd rflns ($I > 3\sigma(I)$)	4831	5071	2290	2309
2θ max, deg	50	50	45	50
no. of params refined	280 + 244 (2 blocks)	421	277	206
R	0.064	0.045	0.071	0.065
R_w	0.076	0.061	0.83	0.106
GOF	1.89	1.87	2.05	3.49

[a] Conditions: Radiation (graphite monochromator), Mo Kα; wavelength, 0.7107 Å; data collected, $+h,+k,\pm l$. [b] $C_{56}H_{56}CuB_9NP_3$. [c] $C_{38}H_{41}Cu_2B_9P_2$. [d] $C_{27}H_{32}CuB_9NO_2P$. [e] $C_{27}H_{51}Cu_3B_{27}N_3O_6\cdot{}^1/_3C_7H_{16}$.

H, 5.27; B, 12.41; P, 7.90; Cu, 16.21. Found: C, 57.94; H, 5.10; B, 11.79; P, 7.44; Cu, 16.11. IR (cm^{-1}): 3071 (m), 2559 (s), 2498 (s), 2320 (w), 1480 (s), 1435 (s), 1097 (s), 1031 (w), 998 (w), 960 (w), 743 (s), 693 (s), 527 (s), 498 (s). ^{1}H NMR (ppm, CD_2Cl_2): 7.22–7.45 (envelope, PPh_3), 2.01 (s, carborane CH). $^{31}P\{^1H\}$ NMR (ppm, 10% CD_2Cl_2/CH_2Cl_2): 7.9 (above 253 K); 4.7 and 10.1 (203 K). $^{11}B\{^1H\}$ NMR (ppm, CH_2Cl_2): −17.4, −19.7, −22.5, −24.2, −29.7, −31.2.

[*closo*-3-(PPh$_3$)-4-(4-(C$_5$H$_4$N)CO$_2$CH$_3$)-3,1,2-CuC$_2$B$_9$H$_{10}$] (5). To a slurry of anhydrous CuCl (1 mmol) and triphenylphosphine (2 mmol) in 20 mL of THF was added a deep purple solution generated by refluxing a slurry of [*nido*-9-(4-(C_5H_4N)CO_2CH_3)-7,8-$C_2B_9H_{11}$] (1 mmol) and 100 mg of NaH in 100 mL of THF for 3 h, resulting in an immediate color change to orange as well as formation of white solids. The reaction mixture was stirred for 24 h at 298 K and filtered over a Celite pad. The orange filtrate was reduced in volume, and heptane was added. The resulting orange crystals were collected and washed with Et_2O, dried in vacuo, and recrystallized from THF/heptane, affording analytically pure product in a yield of 22% (130 mg). Anal. Calcd for $C_{27}H_{32}B_9PNO_2Cu$: C, 54.56; H, 5.43; B, 16.37; P, 5.21; N, 2.36; Cu, 10.69. Found: C, 54.47; H, 5.49; B, 15.44; P, 5.26; N, 2.10; Cu, 10.91. IR (cm^{-1}): 3068 (w), 2959 (w), 2559 (s), 2534 (s), 2524 (s), 2475 (s), 2460 (m), 1736 (s), 1480 (w), 1434 (s), 1290 (s), 1113 (m), 1097 (m), 1024 (w), 750 (m), 696 (s), 530 (m), 514 (m). ^{1}H NMR (ppm, CD_2Cl_2): 8.5 (d, $-NC_5H_4-$), 7.7 (d, $-NC_5H_4-$), 7.2–7.5 (envelope, PPh_3), 4.0 (s, CH_3), 2.5 (s, carborane CH), 2.1 (s, carborane CH). $^{31}P\{^1H\}$ NMR (ppm, 10% C_6D_6/THF): 8.4 (PPh_3). $^{11}B\{^1H\}$ NMR (ppm, THF): −6.7, −16.0, −17.2, −19.5, −22.3, −26.4, −34.7.

[Cu$_3$(μ-H)$_3${C$_2$B$_9$(4-(C$_5$H$_4$N)CO$_2$CH$_3$)}$_3$]·*n*-C$_7$H$_{16}$ (6·*n*-C$_7$H$_{16}$). To a slurry of anhydrous CuCl (1 mmol) in 20 mL of THF was added a deep purple solution generated by deprotonation of [*nido*-9-(4-C_5H_4N)-CO_2CH_3)-7,8-$C_2B_9H_{11}$] with NaH by the procedure described above, resulting in an intense red color as well as formation of white solids. The reaction mixture was stirred at ambient temperature for 20 h and then filtered. The filtrate was repeatedly treated with heptane until precipitation of orange solid ceased. Removal of this solid followed by further treatment of the filtrate with heptane afforded red crystalline product in a yield of 18% (61 mg). IR (cm^{-1}): 3119 (w), 2951 (w), 2557 (s), 2440 (w), 2368 (w), 2281 (w), 2108 (w), 1733 (s), 1434 (s), 1327 (m), 1294 (s), 1113 (s), 1087 (m), 956 (w), 868 (w), 763 (w), 693 (w), 502 (w), 450 (w) cm^{-1}. ^{1}H NMR (ppm, CD_2Cl_2): 8.7 (m, $-NC_5H_4-$), 8.1 (d, $-NC_5H_4-$), 4.0 (s, CH_3), 2.8 (s, carborane CH), 2.0 (s, carborane CH). $^{11}B\{^1H\}$ NMR (ppm, THF): −6.0, −12.6, −19.7, −26.7, −30.7, −34.6. Mass spectrum: base peak at m/e 267; the parent ion was not detected.

Table VII. Positional and Equivalent Isotropic Thermal Parameters for PPN[**3**][a]

atom	x	y	z	$\langle u^2\rangle$
Cu(03)	0.706 46 (6)	0.163 57 (6)	0.691 19 (3)	0.055
P(01)	0.842 51 (13)	0.146 56 (11)	0.738 53 (5)	0.048
C(01)	0.562 5 (5)	0.273 0 (4)	0.693 5 (2)	0.055
C(02)	0.653 1 (5)	0.296 6 (4)	0.656 5 (2)	0.058
B(04)	0.516 9 (6)	0.166 0 (5)	0.689 8 (2)	0.049
B(05)	0.427 0 (6)	0.257 6 (5)	0.672 7 (3)	0.060
B(06)	0.515 5 (7)	0.342 8 (6)	0.652 4 (3)	0.070
B(07)	0.677 9 (6)	0.207 5 (6)	0.624 8 (2)	0.053
B(08)	0.586 6 (6)	0.120 6 (5)	0.643 1 (2)	0.050
B(09)	0.441 3 (6)	0.161 3 (5)	0.639 6 (2)	0.054
B(10)	0.443 5 (7)	0.272 1 (6)	0.616 5 (3)	0.069
B(11)	0.589 6 (7)	0.301 4 (6)	0.607 0 (3)	0.069
B(12)	0.542 8 (7)	0.189 5 (6)	0.598 5 (3)	0.067
C(11)	0.923 5 (3)	0.247 2 (3)	0.755 21 (14)	0.049
C(12)	0.859 9 (3)	0.325 9 (3)	0.763 09 (14)	0.060
C(13)	0.916 0 (3)	0.403 5 (3)	0.778 17 (14)	0.072
C(14)	1.035 8 (3)	0.402 6 (3)	0.785 37 (14)	0.078
C(15)	1.099 5 (3)	0.323 9 (3)	0.777 50 (14)	0.084
C(16)	1.043 3 (3)	0.246 3 (3)	0.762 42 (14)	0.071
C(21)	0.955 5 (4)	0.069 7 (3)	0.719 46 (11)	0.047
C(22)	0.979 9 (4)	−0.013 4 (3)	0.739 02 (11)	0.063
C(23)	1.066 7 (4)	−0.068 9 (3)	0.722 14 (11)	0.072
C(24)	1.129 2 (4)	−0.041 4 (3)	0.685 71 (11)	0.067
C(25)	1.104 8 (4)	0.041 8 (3)	0.666 16 (11)	0.070
C(26)	1.018 0 (4)	0.097 3 (3)	0.683 03 (11)	0.065
C(31)	0.794 9 (3)	0.102 3 (3)	0.790 72 (13)	0.050
C(32)	0.679 2 (3)	0.075 4 (3)	0.794 53 (13)	0.062
C(33)	0.638 5 (3)	0.041 5 (3)	0.833 97 (13)	0.080
C(34)	0.713 5 (3)	0.034 6 (3)	0.869 59 (13)	0.078
C(35)	0.829 2 (3)	0.061 5 (3)	0.865 78 (13)	0.077
C(36)	0.869 9 (3)	0.095 3 (3)	0.826 34 (13)	0.064
P (PPN)	0.270 32 (13)	0.144 78 (11)	0.929 15 (5)	0.044
P (PPN)	0.428 72 (13)	0.291 04 (11)	0.963 15 (5)	0.043
N (PPN)	0.380 6 (4)	0.197 8 (3)	0.946 54 (15)	0.047

[a] Units of $\langle u^2\rangle$ are Å^2. Units of each esd, in parentheses, are those of the least significant digit of the corresponding parameter. Isotropic values are equal to $[1/(8\pi^2)]B_{eq}$.[50]

Collection and Reduction of X-ray Data for PPN[3]. A crystal, obtained from CH_2Cl_2/Et_2O solution, was mounted on a thin glass fiber on a Huber diffractometer. Systematic absences were found for reflections $0k0$, $k = 2n + 1$, and $h0l$, $h + l = 2n + 1$. Unit cell parameters were determined from a least-squares fit of 37 accurately centered reflections (9° < 2θ < 20°). These dimensions and other parameters, including conditions of data collection, are summarized in Table VI. Data were collected in the θ–2θ scan mode to a limit in 2θ of 50°. Three intense reflections, (−2,3,−3), (0,1,−7), and (132), were monitored every 97 reflections to check stability. Intensities of these reflections fluctuated only slightly, ca. ±3%, during the course of the experiment. Of the 9219

Table VIII. Positional and Equivalent Isotropic Thermal Parameters for **4**[a]

atom	x	y	z	$\langle u^2 \rangle$
Cu(01)	0.27341 (5)	0.34089 (3)	0.26324 (3)	0.055
Cu(03)	0.08341 (5)	0.41001 (2)	0.31085 (2)	0.045
P(01)	−0.02415 (10)	0.45615 (5)	0.22307 (5)	0.040
P(02)	0.37513 (11)	0.29754 (5)	0.17475 (5)	0.045
C(01)	0.2207 (4)	0.4618 (2)	0.3959 (2)	0.043
C(02)	0.0825 (1)	0.4419 (2)	0.4257 (2)	0.046
B(04)	0.2914 (5)	0.4012 (2)	0.3568 (2)	0.040
B(05)	0.3530 (5)	0.4256 (3)	0.4424 (3)	0.048
B(06)	0.2151 (5)	0.4557 (3)	0.4857 (2)	0.050
B(07)	0.0426 (5)	0.3645 (3)	0.4102 (2)	0.049
B(08)	0.1819 (5)	0.3323 (2)	0.3665 (2)	0.042
B(09)	0.3277 (5)	0.3423 (2)	0.4244 (3)	0.048
B(10)	0.2766 (5)	0.3772 (3)	0.5047 (3)	0.054
B(11)	0.1019 (5)	0.3904 (3)	0.4956 (2)	0.051
B(12)	0.1706 (5)	0.3204 (3)	0.4587 (3)	0.051
C(11)	0.0500 (2)	0.5316 (1)	0.19535 (15)	0.044
C(12)	−0.0244 (2)	0.58795 (14)	0.18369 (15)	0.059
C(13)	0.0389 (2)	0.64457 (14)	0.16335 (15)	0.072
C(14)	0.1766 (2)	0.64486 (14)	0.15466 (15)	0.074
C(15)	0.2510 (2)	0.58853 (14)	0.16633 (15)	0.080
C(16)	0.1877 (2)	0.53191 (14)	0.18667 (15)	0.064
C(21)	−0.0376 (3)	0.40779 (9)	0.14344 (12)	0.039
C(22)	−0.0456 (3)	0.43547 (9)	0.07643 (12)	0.048
C(23)	−0.0628 (3)	0.39626 (9)	0.01696 (12)	0.058
C(24)	−0.0720 (3)	0.32937 (9)	0.02451 (12)	0.066
C(25)	−0.0640 (3)	0.30169 (9)	0.09153 (12)	0.063
C(26)	−0.0468 (3)	0.34090 (9)	0.15099 (12)	0.052
C(31)	−0.1976 (2)	0.47594 (15)	0.24005 (11)	0.044
C(32)	−0.2258 (2)	0.49709 (15)	0.30748 (11)	0.060
C(33)	−0.3568 (2)	0.51248 (15)	0.32316 (11)	0.064
C(34)	−0.4597 (2)	0.50671 (15)	0.27141 (11)	0.053
C(35)	−0.4315 (2)	0.48556 (15)	0.20397 (11)	0.062
C(36)	−0.3004 (2)	0.47018 (15)	0.18829 (11)	0.059
C(41)	0.2856 (3)	0.22996 (15)	0.13438 (14)	0.047
C(42)	0.3040 (3)	0.20999 (15)	0.06537 (14)	0.071
C(43)	0.2289 (3)	0.15883 (15)	0.03665 (14)	0.084
C(44)	0.1353 (3)	0.12762 (15)	0.07693 (14)	0.074
C(45)	0.1168 (3)	0.14759 (15)	0.14593 (14)	0.074
C(46)	0.1920 (3)	0.19876 (15)	0.17466 (14)	0.061
C(51)	0.5378 (3)	0.26715 (13)	0.20664 (14)	0.046
C(52)	0.5961 (3)	0.21223 (13)	0.17852 (14)	0.059
C(53)	0.7199 (3)	0.19048 (13)	0.20586 (14)	0.072
C(54)	0.7853 (3)	0.22365 (13)	0.26132 (14)	0.079
C(55)	0.7270 (3)	0.27857 (13)	0.28944 (14)	0.082
C(56)	0.6032 (3)	0.30032 (13)	0.26210 (14)	0.064
C(61)	0.4097 (3)	0.34819 (15)	0.10037 (16)	0.049
C(62)	0.5334 (3)	0.34924 (15)	0.06936 (16)	0.063
C(63)	0.5504 (3)	0.38615 (15)	0.00898 (16)	0.093
C(64)	0.4437 (3)	0.42200 (15)	−0.02039 (16)	0.117
C(65)	0.3200 (3)	0.42095 (15)	0.01062 (16)	0.118
C(66)	0.3031 (3)	0.38405 (15)	0.07100 (16)	0.082

[a] See footnote *a* of Table VII.

unique reflections measured, 4831 were considered observed ($I > 3\sigma(I)$) and were used in the subsequent structure analysis. Data were corrected for Lorentz, polarization, and absorption effects. Programs used in this work include locally modified versions of crystallographic programs listed in the reference section.[47] Any redundant data collected were deleted before processing.

Solution and Refinement of the Structure of PPN[3]. Atoms in PPN[3] and also for the three compounds that follow were located by use of the heavy-atom method. All calculations for PPN[3], **4**, **5**, and **6** were performed on the VAX 11/750 crystallographic computer. For all four compounds, scattering factors for hydrogen were obtained from Stewart et al.[48] and for other atoms were taken from ref 49.

Table IX. Positional and Equivalent Isotropic Thermal Parameters for **5**[a]

atom	x	y	z	$\langle u^2 \rangle$
Cu(03)	0.25233 (8)	0.45627 (10)	0.10511 (6)	0.064
P(01)	0.2369 (2)	0.3132 (2)	0.17221 (14)	0.060
N(41)	0.3117 (4)	0.3453 (6)	−0.0326 (4)	0.047
O(41)	0.5140 (5)	0.0117 (6)	−0.0812 (4)	0.094
O(42)	0.3605 (5)	−0.0305 (5)	−0.1215 (4)	0.081
C(11)	0.2073 (4)	0.1903 (6)	0.1183 (3)	0.059
C(12)	0.2733 (4)	0.1050 (6)	0.1093 (3)	0.066
C(13)	0.2478 (4)	0.0184 (6)	0.0623 (3)	0.074
C(14)	0.1563 (4)	0.0171 (6)	0.0243 (3)	0.079
C(15)	0.0903 (4)	0.1024 (6)	0.0333 (3)	0.082
C(16)	0.1158 (4)	0.1890 (6)	0.0803 (3)	0.070
C(21)	0.3481 (6)	0.2797 (5)	0.2273 (4)	0.065
C(22)	0.4268 (6)	0.3520 (5)	0.2263 (4)	0.080
C(23)	0.5141 (6)	0.3283 (5)	0.2666 (4)	0.088
C(24)	0.5227 (6)	0.2323 (5)	0.3078 (4)	0.088
C(25)	0.4440 (6)	0.1600 (5)	0.3089 (4)	0.078
C(26)	0.3567 (6)	0.1837 (5)	0.2686 (4)	0.071
C(31)	0.1424 (6)	0.3202 (6)	0.2337 (4)	0.072
C(32)	0.0942 (6)	0.2272 (6)	0.2570 (4)	0.094
C(33)	0.0227 (6)	0.2393 (6)	0.3043 (4)	0.124
C(34)	−0.0006 (6)	0.3444 (6)	0.3284 (4)	0.139
C(35)	0.0475 (6)	0.4374 (6)	0.3051 (4)	0.130
C(36)	0.1190 (6)	0.4253 (6)	0.2578 (4)	0.101
C(41)	0.4055 (6)	0.3176 (7)	−0.0141 (4)	0.053 (2)*[b]
C(42)	0.4441 (6)	0.2182 (7)	−0.0305 (5)	0.058 (2)*
C(43)	0.3857 (6)	0.1409 (7)	−0.0667 (4)	0.052 (2)*
C(44)	0.2874 (6)	0.1668 (7)	−0.0855 (5)	0.056 (2)*
C(45)	0.2547 (7)	0.2696 (7)	−0.0660 (5)	0.059 (2)*
C(46)	0.4293 (8)	0.0339 (9)	−0.0898 (5)	0.068 (3)*
C(47)	0.3928 (8)	−0.1330 (10)	−0.1512 (6)	0.099 (4)*
C(01)	0.1529 (6)	0.4752 (8)	−0.0106 (5)	0.055 (2)*
C(02)	0.1320 (6)	0.5698 (8)	0.0425 (5)	0.060 (3)*
B(04)	0.2716 (7)	0.4588 (9)	−0.0124 (5)	0.047 (2)*
B(05)	0.2001 (8)	0.5244 (10)	−0.0851 (6)	0.059 (3)*
B(06)	0.1054 (9)	0.5950 (10)	−0.0472 (6)	0.069 (3)*
B(07)	0.2324 (8)	0.6302 (9)	0.0842 (6)	0.059 (3)*
B(08)	0.3319 (8)	0.5624 (10)	0.0424 (6)	0.062 (3)*
B(09)	0.3122 (8)	0.5813 (10)	−0.0512 (6)	0.060 (3)*
B(10)	0.2073 (9)	0.6687 (11)	−0.0731 (7)	0.076 (4)*
B(11)	0.1589 (9)	0.6968 (11)	0.0100 (7)	0.072 (4)*
B(12)	0.2856 (8)	0.6905 (10)	0.0882 (6)	0.063 (3)*

[a] See footnote *a* of Table VII. [b] Asterisks denote an atom refined isotropically.

All carborane hydrogen atoms in PPN[3] were kept in located positions, and all phenyl hydrogen atoms were included in calculated positions, C–H = 1.0 Å, with assigned u values of 0.076 Å^2. Anisotropic thermal parameters were refined for all non-hydrogen atoms. Anomalous dispersion terms were applied to the scattering of Cu and P. A final difference electron density map was essentially featureless, the maximum and minimum peaks being about 0.3 e Å^{-3}. Final positional and thermal parameters for non-hydrogen atoms are given in Table VII.

Collection and Reduction of X-ray Data for 4. A colorless crystal, obtained from CH_2Cl_2/Et_2O as a parallelepiped with faces (010), (0,−1,0), (100), (−1,0,0), (001), and (0,0−1), was mounted on a glass fiber. Unit cell dimensions were determined from a least-squares fit of 23 accurately centered reflections ($9° < 2\theta < 20°$). These, and other parameters, including conditions of data collection, are summarized in Table VI. Data were collected on a Huber diffractometer. Three reflections, (0,−3,4), (142), and (−2,3,−1), were measured every 97 reflections to check stability. There was no appreciable decay. Intensities of these reflections fluctuated only slightly, a maximum of ±5%, during the course of the experiment. A total of 6925 unique reflections were measured. Of these, 5071 were considered observed ($I > 3\sigma(I)$) and were used in the subsequent structure analysis. Other conditions for collection and reduction were the same as those that were applied to PPN[3].

Solution and Refinement of the Structure of 4. In the course of refinement, all C and B atoms of the icosahedral ligand were assigned boron scattering factors and full-matrix least-squares refinement of these atoms led to identification of the carbon atoms. All hydrogen atoms of the $C_2B_9H_{11}$ ligand were located. All hydrogen atoms of phenyl groups were included in calculated positions, C–H = 1.0 Å. The number of

---

(47) Programs: CARESS (Broach, Coppens, Becker, and Blessing), peak profile analysis, Lorentz and polarization corrections; ORFLS (Busing, Martin, and Levy), structure factor calculation and full-matrix least-squares refinement; ABSORB (Coppens, Edwards, and Hamilton), absorption correction calculation; ORTEP (Johnson), figure plotting; SHELX76 (Sheldrick), structure analysis package.

(48) Stewart, R. F.; Davidson, E. R.; Simpson, W. T. *J. Chem. Phys.* **1965**, *42*, 3175.

(49) *International Tables for X-ray Crystallography*; Kynoch: Birmingham, England, 1974; Vol. IV.

(50) Hamilton, W. C. *Acta Crystallogr.* **1959**, *12*, 609.

Table X. Positional Parameters and Equivalent Isotropic Temperature Factors for **6**$\cdot{}^1/_3n$-C_7H_{16}[a]

atom	x	y	z	10^4u[a]
Cu	0.08854 (6)	0.07898 (6)	0.28454 (3)	247 (5)
B(01)	0.3080 (6)	0.0249 (6)	0.2777 (3)	28 (8)
B(02)	0.2276 (6)	−0.0257 (6)	0.3223 (3)	25 (7)
B(03)	0.3116 (6)	0.0879 (6)	0.3273 (3)	26 (7)
B(04)	0.3294 (6)	0.1352 (6)	0.2709 (3)	27 (8)
B(05)	0.2581 (6)	0.0531 (6)	0.2305 (3)	26 (8)
B(06)	0.1937 (6)	−0.0486 (6)	0.2626 (3)	25 (7)
C(07)	0.2005 (5)	0.0547 (5)	0.3365 (2)	23 (6)
C(08)	0.2568 (5)	0.1428 (5)	0.3088 (2)	49 (6)
B(09)	0.2256 (5)	0.1281 (5)	0.2531 (3)	20 (7)
B(10)	0.1436 (6)	0.0157 (6)	0.2442 (3)	22 (7)
B(11)	0.1271 (5)	−0.0270 (5)	0.3037 (3)	21 (7)
C(91)	0.1947 (5)	0.1936 (5)	0.1828 (2)	25 (6)
C(92)	0.2063 (5)	0.2623 (5)	0.1538 (2)	26 (7)
C(93)	0.2704 (5)	0.3488 (5)	0.1651 (3)	26 (7)
C(94)	0.3203 (5)	0.3648 (5)	0.2057 (2)	23 (6)
C(95)	0.3040 (5)	0.2939 (5)	0.2338 (2)	22 (6)
C(96)	0.2846 (5)	0.4214 (5)	0.1316 (3)	28 (7)
C(97)	0.3848 (6)	0.5633 (6)	0.1019 (3)	45 (8)
N(91)	0.2429 (4)	0.2095 (4)	0.2226 (2)	19 (6)
O(91)	0.2310 (4)	0.4132 (4)	0.1027 (2)	36 (5)
O(92)	0.3634 (4)	0.4953 (4)	0.1370 (2)	36 (5)
C(38S)	0.6590 (16)	0.2387 (16)	0.2356 (8)	33 (6)*
C(41S)	0.618 (3)	0.222 (3)	0.2844 (15)	101 (13)*
C(39S)	0.6667	0.3331	0.2293 (16)	204 (19)*

[a] $u_{eq} = [1/(6\pi^2)]\sum\sum\beta_{ij}a_ia_j$ (Å^2). [b] Asterisks denote atoms refined with isotropic temperature factors.

parameters refined was 421, including positional and anisotropic thermal parameters for all non-hydrogen atoms and positional parameters for all hydrogen atoms of the icosahedron. All hydrogen atoms of the icosahedron were assigned a thermal parameter of 0.06 (u). All hydrogen atoms of phenyl groups were assigned a thermal parameter of 0.08. Anomalous dispersion terms were applied to scattering of Cu and P. Final positional and thermal parameters are given in Table VIII. A final difference electron density map was essentially featureless, the maximum and minimum peaks being about 0.3 e Å^{-3}.

Collection and Reduction of X-ray Data for 5. An orange crystal, obtained from THF/Et_2O solution, was mounted on a thin glass fiber on a Huber diffractometer. Systematic absences were found for reflections $0k0$, $k = 2n + 1$, and for $h0l$, $h + l = 2n + 1$. Unit cell parameters were determined from a least-squares fit of 27 accurately centered reflections (9.5° $< 2\theta <$ 20.2°). These dimensions and other parameters, including conditions of data collection, are summarized in Table VI. Three intense reflections, (1,−2,3), (016), and (3,0,−2), were monitored every 97 reflections to check stability. Intensities of these reflections fluctuated only slightly, ca. ±4%, during the course of the experiment. Of the 4078 unique reflections measured, 2290 were considered observed ($I > 3\sigma(I)$) and were used in the subsequent structure analysis. Other conditions for data collection and reduction were the same as those applied to PPN[**3**].

Solution and Refinement of the Structure of 5. For hydrogen atoms of the C_2B_9 cage, an isotropic u value of 0.075 Å^2 was assigned and positional parameters were refined. All phenyl hydrogen atoms in triphenylphosphine and aromatic and methyl hydrogen atoms in methyl isonicotinate were included in calculated positions, C–H = 1.0 Å, with assigned u values of 0.10, 0.08, and 0.10 Å^2, respectively. With the exception of the atoms of the C_2B_9 fragment and the C atoms of the methyl isonicotinate, anisotropic thermal parameters were refined for all non-hydrogen atoms. Phenyl groups of triphenylphosphine for **3**, **4**, and **5** and PPN for **3** were constrained to be rigid hexagons, C–C = 1.395 Å and C–C–C = 120°. Anomalous dispersion terms were applied to the scattering of Cu and P. A final difference electron density map was essentially featureless, the maximum and minimum peaks being about 0.5 e Å^{-3}. Final positional and thermal parameters for non-hydrogen atoms are given in Table IX.

Collection and Reduction of X-ray Data for 6$\cdot n$-C_7H_{16}**.** A red crystal, obtained from THF/heptane solution, was mounted on a thin glass fiber on a Picker FACS-1 diffractometer modified by Professor C. E. Strouse of this department. Systematic absences were found for reflections for which $-h + k + l \neq 3n$. Unit cell parameters were determined from a least-squares fit of 34 accurately centered reflections (9.7° $< 2\theta <$ 18.6°). These dimensions and other parameters, including conditions of data collection, are summarized in Table VI. Data were collected at 128 K. Three intense reflections, (2,−3,5), (125), and (4,3,−8), were monitored every 97 reflections to check stability. Intensities of these reflections fluctuated only slightly, ca. ±6%, during the course of the experiment. Of the 3065 unique reflections measured, 2309 were considered observed ($I > 3\sigma(I)$) and were used in the subsequent structure analysis. Other conditions for collection and reduction were the same as those applied to PPN[**3**]. The assignment of the space group $R\bar{3}$ was confirmed by successful refinement of the data.

Solution and Refinement of the Structure of 6$\cdot n$-C_7H_{16}**.** With the exception of those of the methyl group and of the disordered heptane molecule which occupies a position near a 3-fold axis, all hydrogen atoms were located and were included in structure factor calculations with an assigned B value of 2.0 Å^2. Hydrogen parameters were not refined. Anomalous dispersion terms were applied to the scattering of Cu. A final difference electron density map was essentially featureless, the maximum peaks being about 0.7 e Å^{-3}. All of the larger peaks were in the vicinity of the heptane molecule. Final positional and thermal parameters for non-hydrogen atoms are given in Table X.

Other Physical Measurements. The ^{1}H (200.133 MHz) and $^{31}P\{^1H\}$ (81.02 MHz) FT NMR spectra were recorded on a Bruker WP-200 instrument equipped with a deuterium lock and a B-VT-1000 temperature controller for variable-temperature measurement. The ^{11}B FT NMR spectra were recorded at 160.463 MHz on a Bruker AM-500 instrument. Proton chemical shifts were referenced to residual solvent protons (CD_2Cl_2, 5.32 ppm; C_6D_6, 7.15 ppm; vs Me_4Si). Phosphorus and boron chemical shifts were externally referenced to 85% H_3PO_4 and $BF_3{\cdot}OEt_2$, respectively. All chemical shifts downfield of the reference are designated as positive. IR spectra were recorded as KBr pellets on a Beckman FT-1100 Fourier transform spectrophotometer. Elemental analyses were performed by Galbraith Laboratories, Knoxville, TN.

Acknowledgment. We gratefully acknowledge financial support provided by the Office of Naval Research. We also thank Dr. A. Varadarajan in this group for informative discussions.

Registry No. PPN[**3**], 109333-83-7; **4**, 109333-84-8; **5**, 113725-90-9; **6**, 110509-33-6; **6**$\cdot{}^1/_3n$-C_7H_{16}, 113725-91-0; [$Tl_2C_2B_9H_{11}$], 97102-40-4; CuCl, 7758-89-6; [*nido*-9-(4-(C_5H_4N)CO_2CH_3)-7,8-$C_2B_9H_{11}$], 110433-08-4; Cu, 7440-50-8.

Supplementary Material Available: Tables of hydrogen atom positional and thermal parameters, anisotropic thermal parameters, and interatomic distances and angles (25 pages); listings of observed and calculated structure factors (66 pages). Ordering information is given on any current masthead page.